Title

Bioengineering Novel Chimeric microRNA-34a for Prodrug Cancer Therapy: High-Yield Expression and Purification, and Structural and Functional Characterization

Journal

Journal of Pharmacology and Experimental Therapeutics, 354(2)

ISSN

0022-3565

Authors

Wang, Wei-Peng
Ho, Pui Yan
Chen, Qiu-Xia
et al.

Publication Date

2015-08-01

DOI

10.1124/jpet.115.225631

Peer reviewed

1521-0103/354/2/131–141$25.00
THE JOURNAL OF PHARMACOLOGY AND EXPERIMENTAL THERAPEUTICS

http://dx.doi.org/10.1124/jpet.115.225631
J Pharmacol Exp Ther 354:131–141, August 2015

The Journal of PHARMACOLOGY And Experimental Therapeutics

Bioengineering Novel Chimeric microRNA-34a for Prodrug Cancer Therapy: High-Yield Expression and Purification, and Structural and Functional Characterization[S]

Wei-Peng Wang, Pui Yan Ho, Qiu-Xia Chen, Balasubrahmanyam Addepalli, Patrick A. Limbach, Mei-Mei Li, Wen-Juan Wu, Joseph L. Jilek, Jing-Xin Qiu, Hong-Jian Zhang, Tianhong Li, Theodore Wun, Ralph DeVere White, Kit S. Lam, and Ai-Ming Yu

Department of Biochemistry and Molecular Medicine (W.-P.W., P.Y.H., Q.-X.C., M.-M.L., W.-J.W., J.L.J., K.S.L., A.-M.Y.), Division of Hematology Oncology (T.L., T.W., K.S.L.) and Department of Urology (R.D.W.), School of Medicine, University of California–Davis, Sacramento, California; Rieveschl Laboratories for Mass Spectrometry, Department of Chemistry, University of Cincinnati, Cincinnati, Ohio (B.A., P.A.L.); Department of Pathology, Roswell Park Cancer Institute, Buffalo, New York (J.-X.Q.); and Center of Drug Metabolism and Pharmacokinetics, College of Pharmaceutical Sciences, Soochow University, Suzhou, Jiangsu, China (W.-P.W., H.-J.Z.)

Received April 29, 2015; accepted May 27, 2015

ABSTRACT

Development of anticancer treatments based on microRNA (miRNA/miR) such as miR-34a replacement therapy is limited to the use of synthetic RNAs with artificial modifications. Herein, we present a new approach to a high-yield and large-scale biosynthesis, in *Escherichia coli* using transfer RNA (tRNA) scaffold, of chimeric miR-34a agent, which may act as a prodrug for anticancer therapy. The recombinant tRNA fusion pre–miR-34a (tRNA/mir-34a) was quickly purified to a high degree of homogeneity (>98%) using anion-exchange fast protein liquid chromatography, whose primary sequence and post-transcriptional modifications were directly characterized by mass spectrometric analyses. Chimeric tRNA/mir-34a showed a favorable cellular stability while it was degradable by several ribonucleases. Deep sequencing and quantitative real-time polymerase chain reaction studies revealed that tRNA-carried pre–miR-34a was precisely processed to mature miR-34a within human carcinoma cells, and the same tRNA fragments were produced from tRNA/mir-34a and the control tRNA scaffold (tRNA/MSA). Consequently, tRNA/mir-34a inhibited the proliferation of various types of human carcinoma cells in a dose-dependent manner and to a much greater degree than the control tRNA/MSA, which was mechanistically attributable to the reduction of miR-34a target genes. Furthermore, tRNA/mir-34a significantly suppressed the growth of human non–small-cell lung cancer A549 and hepatocarcinoma HepG2 xenograft tumors in mice, compared with the same dose of tRNA/MSA. In addition, recombinant tRNA/mir-34a had no or minimal effect on blood chemistry and interleukin-6 level in mouse models, suggesting that recombinant RNAs were well tolerated. These findings provoke a conversation on producing biologic miRNAs to perform miRNA actions, and point toward a new direction in developing miRNA-based therapies.

Introduction

MicroRNAs are integrated into a large family of genomically encoded noncoding RNAs (ncRNAs) and play a critical role in controlling cancer cell proliferation, apoptosis and invasion, and tumor initiation and progression (Kasinski and Slack, 2011; Bader, 2012), as well as drug disposition (Yu, 2009; Ingelman-Sundberg et al., 2013) and pathogenesis of other diseases (Yao and Li, 2015). MicroRNA (miRNA or miR) biologic functions contribute to the development of novel anticancer treatments, and several miRNA-based therapies are under or moving toward clinical trials. In particular, oncogenic miRNAs (e.g., miR-10b) are upregulated in cancer cells and may be targeted to achieve the control of cancer cell proliferation and tumor growth (Ma et al., 2007). Furthermore, tumor suppressive miRNAs (e.g., miR-34a) are showing a loss-of-function in cancerous tissues and may be reintroduced into cancer cells to suppress tumor progression (He

This work was supported in part by the National Institutes of Health National Cancer Institute [Grant 1U01-CA175315]; and the National Science Foundation [Grant CHE 1212625].
W.-P.W., P.Y.H., Q.-X.C. contributed equally to this study.
dx.doi.org/10.1124/jpet.115.225631.
[S] This article has supplemental material available at jpet.aspetjournals.org.

ABBREVIATIONS: CDK6, cyclin-dependent kinase 6; EU, endotoxin units; FPLC, fast protein liquid chromatography; GAPDH, glyceraldehyde-3-phosphate dehydrogenase; HPLC, high-performance liquid chromatography; IL-6, interleukin-6; LAL, Limulus amebocyte lysate; LPS, lipopolysaccharide; miR or miRNA, microRNA; mir, pre-miRNA; ncRNA, noncoding RNA; pre-miR, pre-microRNA; qRT-PCR, quantitative real-time polymerase chain reaction; SIRT1, sirtuin-1; tRNA, transfer RNA; tRF, tRNA fragment; tRNA/mir, tRNA fusion pre-miRNA; tRNA/mir-34a, tRNA fusion pre–miR-34a; tRNA/MSA, Sephadex aptamer tagged methionyl-tRNA.

et al., 2007; Welch et al., 2007). The later approach, namely "miRNA replacement therapy," is distinguished from the former miRNA antagonism strategy. The miRNAs or pre-miRNAs used in miRNA replacement therapy have the same sequences as genomically-encoded miRNAs or pre-miRNAs, and therefore are unlikely to produce "off-target" effects. Because miRNAs are normal constituents of healthy cells, reintroduction of therapeutic miRNAs is unlikely to cause major toxicity (Bader, 2012).

Human miR-34a is one of the most promising tumor suppressive miRNAs for cancer treatment. Loss of miR-34a expression has been documented in various tumors, including lung, prostate, breast, pancreas, liver, colon, kidney, bladder, skin, esophagus, brain, cervix, ovary, urothelium, and lymphoid systems (see review in Bader, 2012). The biogenesis of miR-34a is directly controlled by tumor protein p53 at the transcriptional level (Chang et al., 2007; He et al., 2007), and an ectopic expression of miR-34a leads to a dramatic reprogramming of target genes, such as cyclin-dependent kinase 6 (CDK6), hepatocyte growth factor receptor MET, platelet-derived growth factor receptor-α (*PDGFRA*), and GTPase KRAS, and consequently inhibits cancer cell proliferation, induces cell cycle arrest, and enhances apoptosis (Chang et al., 2007; He et al., 2007; Sun et al., 2008; Yamakuchi et al., 2008; Li et al., 2009; Kasinski and Slack, 2012). Meanwhile, miR-34a can stimulate endogenous p53 activity in a positive feedback-loop by targeting the NAD-dependent deacetylase sirtuin-1 (SIRT1) that deactivates p53, and the transcriptional repressor Yin Yang 1 (YY1) that binds to p53 and promotes p53 ubiquitination and degradation (Yamakuchi et al., 2008). Moreover, miR-34a suppresses a clonogenic expansion, tumor regeneration, and metastasis through targeting CD44 and cancer stem cells or tumor-initiating cells (Liu et al., 2011). The anticancer activity of miR-34a has been nicely demonstrated in various human cancer cells in vitro, including lung, liver, pancreas, colon, brain, skin, prostate, bone, ovary, as well as lymphoma and leukemia. Although the performance of miR-34a replacement therapy in animal models depends heavily on the delivery system, a number of successful examples have illustrated the effectiveness of miR-34a in inhibiting progression of many types of xenograft tumors, including non–small-cell lung cancer (Wiggins et al., 2010; Kasinski and Slack, 2012), prostate cancer (Liu et al., 2011), pancreatic cancer (Pramanik et al., 2011), and lymphomas (Craig et al., 2012). As a result, MRX34 (Mirna Therapeutics, Austin, TX), a liposome-formulated miR-34a, has entered phase I clinical trials for the treatment of unresectable primary liver cancer (Kelnar et al., 2014).

Nevertheless, research on miRNA pharmacology and therapeutics rely primarily on the use of synthetic RNAs [e.g., miRNA-mimics and antagomirs, and pre-miRNAs (mir)] and recombinant DNA agents (e. g., viral or nonviral vector-based miRNA or "decoy" antisense RNA expression plasmids). The use of DNA materials may complicate the RNA-based processes, and this approach also relies on the host cells or organisms to transcribe the gene to miRNA precursors before the generation of mature miRNAs. Although organic synthesis of oligonucleotides may be automated, a multimilligram dose of 22-nt double-stranded miRNA-mimics projected for in vivo testing or therapy is very costly. In addition, it is unknown how artificial modifications may alter the folding, biologic activities, and safety profiles, even though synthetic miRNAs exhibit some favorable pharmacokinetic properties, such as a longer half-life.

Motivated by the idea of deploying biologic RNAs to perform RNA actions for pharmacotherapy, we aimed to bioengineer pre-miRNA agents in common strains of bacteria on a large scale using the transfer RNA (tRNA) scaffold (Ponchon and Dardel, 2007; Ponchon et al., 2009; Nelissen et al., 2012). We hypothesized that the tRNA fusion pre-miRNA (tRNA/mir) could act as a prodrug where pre-miRNA might be selectively processed to mature miRNA in human cells, and tRNA scaffold would be metabolized or degraded to tRNA fragments (tRFs). In contrast to a low-yield production of pre–miR-27b (Li et al., 2014), we present herein an optimal expression and rapid purification of multimilligrams of tRNA fusion pre–miR-34a (tRNA/mir-34a) from 1 liter of bacterial culture in a research laboratory setting. The molecular weight, primary sequence, and post-transcriptional modifications of recombinant tRNA/mir-34a were directly characterized by mass spectrometry studies. Furthermore, unbiased deep-sequencing study and targeted quantitative real-time polymerase chain reaction (qRT-PCR) analyses showed that tRNA-carried pre–miR-34a was indeed processed precisely into mature miR-34a in human carcinoma cells, leading to a 70- to 100-fold increase in cellular miR-34a levels. Consequently, tRNA/mir-34a significantly suppressed the protein levels of miR-34a target genes (e.g., CDK6, SIRT1, and MET) and proliferation of human lung (A549 and H460) and liver (HepG2 and Huh-7) cancer cells in vitro in a dose-dependent manner, compared with the control Sephadex aptamer tagged methionyl-tRNA scaffold (tRNA/MSA). In addition, we demonstrated that recombinant tRNA/mir-34a was well tolerated in animal models, and remarkably repressed A549 and HepG2 xenograft tumor growth in vivo. These findings indicate that biologic RNA agents engineered in bacteria may serve as a new category of RNA agents for drug discovery as well as basic and translational research.

Materials and Methods

Lipofectamine 2000, Trizol reagent, and BCA Protein Assay Kit were purchased from Thermo Fisher Scientific Inc. (Waltham, MA). Radioimmunoprecipitation assay lysis buffer was bought from Rockland Immunochemicals (Limerick, PA), and the complete protease inhibitor cocktail was purchased from Roche Diagnostics (Mannheim, Germany). The antibodies against CDK6 (C-21), SIRT1 (H-300), Met (C-28), and glyceraldehyde-3-phosphate dehydrogenase (GAPDH) were purchased from Santa Cruz Biotechnology (Dallas, TX), and peroxidase goat anti-rabbit IgG was from Jackson ImmunoResearch (West Grove, PA). Enhanced chemiluminescent substrate and polyvinylidene fluoride membranes were bought from Bio-Rad (Hercules, CA). All other chemicals and organic solvents of analytical grade were purchased from Sigma-Aldrich (St. Louis, MO) or Thermo Fisher Scientific (Waltham, MA).

Bacterial Culture. All *Escherichia coli* stains were cultured at 37°C in LB broth supplemented with 100 μg/ml ampicillin. DH5α and TOP10 (Life Technologies, Grand Island, NY) were used for cloning as well as screening for recombinant ncRNA expression. BL21 (Sigma-Aldrich) and HST08 (Clontech Laboratories, Mountain View, CA) were also used to screen ncRNA accumulation. HST08 was identified and used for large scale production of recombinant ncRNAs.

Human Cell Culture. The human carcinoma cell lines HepG2, Huh-7, A549, and H460 were purchased from American Type Culture

Collection (Manassas, VA). HepG2 cells were cultured in Eagle's minimal essential medium, A549, and H460 cells in RPMI 1640 medium, and Huh-7 cells in Dulbecco's modified Eagle's medium supplemented with 10% fetal bovine serum (Gibco/Life Technologies), at 37°C in a humidified atmosphere containing 5% CO_2. Cells in the logarithmic growth phase were used for experiments.

Prediction of RNA Secondary Structure. The secondary structures of various sizes of human pre–miR-34a, tRNA scaffold, and the chimeric ncRNAs were predicted using CentroidFold (http://www.ncrna.org/centroidfold), CentroidHomfold (http://www.ncrna.org/centroidhomfold), and RNAstructure (http://rna.urmc.rochester.edu/RNAstructureWeb/Servers/Predict1/Predict1.html).

Construction of tRNA/mir-34a Expression Plasmids. The DNA fragments encoding 112-nt and 129-nt human pre–miR-34a (miRBase ID: MI0000268) were amplified from human genomic DNA by PCR using the primers 5′-AGT AAT TTA CGT CGA CGG CCA GCT GTG AGT GTT TCT TTG G-3′ and 5′-CGG CCG CAA CCA TCG ACG TCT GGG CCC CAC AAC GTG CAG CAC TT-3′, and 5′-AGT AAT TTA CGT CGA CGT GGA CCG GCC AGC TGT GAG TGT T-3′ and 5′-CGG CCG CAA CCA TCG ACG TCA TCT TCC CTC TTG GGC CCC ACA ACG-3′ (IDT, Coralville, IA), respectively. The amplicons were inserted into the pBSMrnaSeph vector (kindly provided by Dr. Luc Ponchon, Université Paris Descartes; Ponchon et al., 2009) linearized with SalI-HF and AatII (New England Biolabs, Ipswich, MA). Target tRNA/mir-34a expression plasmids were confirmed by sequencing analyses at UC Davis Genome Center.

Expression of Recombinant ncRNAs in *E. coli*. Recombinant ncRNAs were expressed in HST08 as described (Ponchon and Dardel, 2007; Ponchon et al., 2009; Li et al., 2014). Total RNAs were isolated using the Tris-HCl–saturated phenol extraction method, quantitated with a NanoDrop 2000 spectrophotometer (Thermo Fisher Scientific), and analyzed by denaturing urea (8 M) PAGE (8%) to assess the expression of recombinant ncRNAs. We usually loaded 0.2–1.0 μg RNAs per lane for the urea-PAGE analysis. The single-stranded RNA ladder and small interfering RNA marker were purchased from New England Biolabs. Images were acquired with a ChemiDo MP Imaging System (Bio-Rad), and intensities of bands were used to provide a rough estimation of relative levels of recombinant ncRNAs present in the total RNAs.

Affinity Purification of Recombinant ncRNAs. Purification of Sephadex aptamer-tagged ncRNAs using Sephadex G-100 beads (Sigma-Aldrich) was conducted as reported (Ponchon et al., 2009; Li et al., 2015), and RNA fractions were analyzed by urea-PAGE.

Fast Protein Liquid Chromatography Purification of Recombinant ncRNAs. Recombinant tRNA/mir-34a was purified from total RNAs on a UNO Q6 anion-exchange column (Bio-Rad) using a NGC Quest 10 Plus Chromatography fast protein liquid chromatography (FPLC) system (Bio-Rad). After the samples were loaded, the column was first equilibrated with buffer A (10 mM sodium phosphate, pH 7.0) at a flow rate 6.0 ml/min for 0.5 minutes, followed by a gradient elution at the same flow rate, 0–56% buffer B (buffer A + 1 M sodium chloride) in 0.5 minute, 56% buffer B for 2 minutes, 56–65% buffer B in 10 minutes, and then 100% buffer B for 2 minutes, 100–0% buffer B in 0.5 minutes, and 100% buffer A for 5 minutes. The salt gradient elution condition for the control tRNA/MSA was essentially the same as reported (Li et al., 2014). FPLC traces were monitored at 260 nm using a UV/Vis detector. Peak areas were also used to estimate the relative levels of recombinant ncRNAs within the total RNAs, which were consistent with those determined by urea-PAGE analyses. After being analyzed by urea-PAGE, the fractions containing pure ncRNAs were pooled. Recombinant ncRNAs were precipitated with ethanol, reconstituted with nuclease-free water, and then desalted and concentrated with Amicon Ultra Centrifugal Filters (2-ml, 30 kDa; EMD Millipore, Billerica, MA). The quantity of ncRNAs was determined using a NanoDrop 2000 spectrophotometer. The quality was validated by PAGE and high-performance liquid chromatography (HPLC) analysis before other experiments.

HPLC Analysis of Purified ncRNAs. HPLC analysis was conducted using an XBridge OST C_{18} column (2.1 × 50 mm, 2.5-μm particle size; Waters, Milford, MA) on a Shimadzu LC-20AD HPLC system. The flow rate was 0.2 ml/min, and the column was maintained at 60°C. Mobile phase A consisted of 8.6 mM TEA and 100 mM hexafluoroisopropanol (pH 8.3) in water, and mobile phase B consisted of 8.6 mM TEA and 100 mM hexafluoroisopropanol in methanol. The LC gradient was as follows: 0–1 minute, 16% mobile phase B; 21 minutes, 22% mobile phase B. RNA was monitored at 260 nm using a photodiode array detector.

Removal and Detection of Endotoxin. Endotoxin was further removed from FPLC-purified ncRNAs using the CleanAll DNA/RNA Clean-up Kit (Norgen Biotek, Thorold, ON, Canada) and Endotoxin-free Water (Lonza, Walkersville, MD), as instructed by the manufacturer. Endotoxin activities in total RNAs as well as the FPLC-purified and CleanAll Kit-processed ncRNA samples were determined using the Pyrogent-5000 kinetic Limulus amebocyte lysate (LAL; Lonza) assay by following the instructions. In particular, a SpectraMax3 plate reader (Molecular Devices, Sunnyvale, CA) was used to measure turbidity at a 340-nm wavelength. Provided endotoxin standards were used to generate a standard curve, and endotoxin levels in RNA samples were expressed in endotoxin units (EU)/μg RNA.

Electrospray Ionization–Mass Spectrometry Analysis of Intact Recombinant ncRNAs. The procedures described by Taucher and Breuker (2010) were followed. The instrumental settings were optimized by automatic tuning with poly-d$(T)_{80}$. The mass spectra were acquired in negative ion mode using a Thermo LTQ XL-ion trap mass spectrometer over an m/z range of 600–2000. Electrospray ionization mass spectra of intact ncRNAs were deconvoluted using ProMass software for Xcalibur (version 2.8 rev. 2) (Novatia, Newtown, PA) to determine the average molecular weights of recombinant RNAs.

Nucleoside Analysis by Liquid Chromatography Coupled with UV and Mass Spectrometry Detection. The hydrolysates were prepared with Nuclease P1 (Sigma-Aldrich), snake venom phosphodiesterase (Worthington Biochemicals Lakewood, Lakewood, NJ), and Antarctic Phosphatase (New England Biolabs), resolved on a 5-μm, 2.1 mm × 250 mm Supelcosil LC-18-S column using a Hitachi D-7000 HPLC system, and analyzed by a diode array detector and a Thermo LTQ-XL ion trap mass spectrometer, as described by Russell and Limbach (2013).

RNA Mapping by Liquid Chromatography–Tandem Mass Spectroscopy. RNA mapping and assignment of modifications using a Thermo Surveyor HPLC system coupled to a Thermo LTQ XL ion trap mass spectrometer and a Thermo Micro AS autosampler after the digestion with RNase T1 (Roche, Indianapolis, IN) and bacterial alkaline phosphatase (Worthington Biochemical Corporation) were carried out as described (Krivos et al., 2011). Collision-induced dissociation tandem mass spectrometry was used to obtain sequence information from the RNase digestion products.

Susceptibility to RNases. Recombinant ncRNAs were digested by individual RNases in provided buffer or HEPES (100 mM KCl, 5 mM $MgCl_2$, 10 mM HEPES, pH 7.4) at 37°C for 1 hour. In particular, 12 μg ncRNAs were incubated with 1 μg/ml human recombinant RNase I (Novoprotein, Summit, NJ), 12 μg ncRNAs with 10 μg/ml Human Recombinant Angiogenin (R&D Systems, Minneapolis, MN), 1 μg ncRNAs with 1 IU of recombinant Dicer (Genlantis, San Diego, CA), 6 μg ncRNAs with 5 IU of bacterial RNase III (Life Technologies), and 5 μg ncRNAs with 5 IU of RNase R (Epicentre, Madison, WI). Likewise, 4 μg RNA was formulated with 0.64 μl in vivo–jetPEI (Polyplus Transfection, New York, NY) delivery agent to a 5% final glucose concentration, and then added to OptiMEM with or without 1 μl human serum (Thermo Fisher Scientific) to a 100 μl volume and incubated at 37°C for 20 minute. The digestion products were analyzed by 8% urea-PAGE.

qRT-PCR. Total RNA was isolated from cells using Direct-zol RNA MiniPrep Kit (Zymo Research, Irvine, CA), and reverse transcribed with NxGen M-MuLV Reverse Transcriptase (Lucigen,

Middleton, WI) and stem-loop primer 5′-GTC GTA TCC AGT GCA GGG TCC GAG GTA TTC GCA CTG GAT ACG ACA CAA CC-3′ for miR-34a, or iScript reverse-transcription Supermix (Bio-Rad) for chimeric ncRNAs, pre–miR-34a, and U6. qRT-PCR was conducted with qRT-PCR Master Mix (New England Biolabs) on a CFX96 Touch real-time PCR system (Bio-Rad), as described (Bi et al., 2014; Li et al., 2014). The primers were as follows: 5′-GGC TAC GTA GCT CAG TTG GT-3′ (forward) and 5′-TGG TGG CTA CGA CGG GAT TC-3′ (reverse) for chimeric ncRNAs; 5′-GGC CAG CTG TGA GTG TTT CTT TGG-3′ (forward) and 5′-GGG CCC CAC AAC GTG CAG-3′ (reverse) for pre-miRNA mir-34a; 5′-CGC GCT GGC AGT GTC TTA GCT-3′ (forward) and 5′-GTG CAG GGT CCG AGG T-3′ (reverse) for mature miR-34a; and 5′-CTC GCT TCG GCA GCA CA-3′ (forward), and 5′-AAC GCT TCA CGA ATT TGC GT-3′ (reverse) for U6. The relative expression was calculated by using the comparative threshold cycle (Ct) method with the formula $2^{-\Delta\Delta Ct}$.

Small RNA Library Construction. Total RNAs were isolated with Trizol reagent (Invitrogen) from A549 cells harvested at 48 hours post-treatment with highly purified ncRNAs or Lipofectamine 2000 (Life Technologies) itself, and the small RNA library was generated using the Illumina Truseq Small RNA Preparation Kit (Illumina, San Diego, CA) according to the instructions.

Deep Sequencing and Data Analysis. The purified cDNA library was used for cluster generation on Illumina's Cluster Station and then sequenced on Illumina GAIIx following vendor's instructions. Raw sequencing reads (40 nt) were obtained using Illumina's Sequencing Control Studio software version 2.8 (SCS v2.8) following real-time sequencing image analysis and base-calling by Illumina's Real-Time Analysis version 1.8.70 (RTA v1.8.70). The extracted sequencing reads were used for the standard sequencing data analysis by following a proprietary pipeline script, ACGT101-miR v4.2 (LC Sciences, Houston, TX).

Immunoblot Analysis. The cell lysates were prepared using a radioimmunoprecipitation assay buffer with the cOmplete Protease Inhibitor Cocktail (Roche, Nutley, NJ). Protein concentrations were determined using the BCA Protein Assay Kit (Thermo Fisher Scientific). Proteins were separated on a 10% SDS-PAGE gel and electrotransferred onto polyvinylidene fluoride membranes using Trans-Blot Turbo Transfer System (Bio-Rad). Membranes were incubated with CDK6 (C-21), SIRT1 (H-300), or Met (C-28) rabbit polyclonal antibody (Santa Cruz Biotechnology) and subsequently with a peroxidase goat anti-rabbit IgG (Jackson ImmunoResearch). The membranes were then incubated with Clarity Western enhanced chemiluminescent substrates (Bio-Rad) and visualized with the ChemiDoc MP Imaging System (Bio-Rad).

Cytotoxicity. The effects of tRNA/mir-34a on the proliferation of cancer cells were determined using an MTT assay, as described (Pan et al., 2013; Li et al., 2015). Cells were seeded in 96-well plates at 3000 or 5000 cells per well, and transfected with various concentrations of tRNA/mir-34a using Lipofectamine 2000 for 72 hours. Cells transfected with the same doses of tRNA/MSA or Lipofectamine 2000 were used as controls. The EC_{50} and Hill slope values were estimated by fitting the data to a normalized inhibitory dose-response model (Prism; GraphPad Software, San Diego, CA).

Xenograft Tumor Mouse Models. All animal procedures were approved by the Institutional Animal Care and Use Committee at University of California–Davis. A549 and HepG2 cells were collected, counted, and mixed with Matrigel (BD Biosciences, San Jose, CA) in a 1:1 ratio by volume. Cells (5×10^6) in 100 μl of medium/Matrigel solution were injected subcutaneously into the lower back region of 5- to 6-week-old male nude mice (The Jackson Laboratory, Bar Harbor, ME). Tumor volumes were measured with a caliper and calculated according to the formula: tumor volume (mm^3) = 0.5 × [length (mm) × width^2 (mm^2)]. Recombinant tRNA/mir-34a and control tRNA/MSA were formulated with in vivo–jetPEI (Polyplus Transfection) and administered intratumorally once tumors reached 150–200 mm^3. Tumors were collected, fixed in 10% formalin, and cut for histologic verification by pathologist.

Safety Profiles in Mouse Models. Male BALB/c mice at five to six weeks of age (The Jackson Laboratory) were administered intravenously via tail vein with 100 μg of ncRNAs formulated with in vivo-jetPEI (Polyplus Transfection). Separate groups of animals were treated with in vivo-jetPEI vehicle as a negative control or 20 μg of lipopolysaccharide (LPS) as a positive control for cytokine induction (Wiggins et al., 2010; Bodeman et al., 2013; Wang et al., 2015). Blood was collected at various time points and serum was isolated using the serum separator (BD Biosciences). Serum cytokine interleukin-6 (IL-6) levels were quantitated using a mouse IL-6 assay kit (Pierce/Thermo Scientific) on a SpectraMax M3 Multi-Mode Spectrophotometer (Molecular Devices), and mouse blood chemistry profiles were determined at the Comparative Pathology Laboratory at UC Davis.

Statistical Analysis. All data were presented as mean ± S.D. According to the number of groups and variances, data were analyzed with unpaired Student's t test, or one-way or two-way analysis of variance (GraphPad Prism). Any difference was considered as significant if the probability was less than 0.05 ($P < 0.05$).

Results

Chimeric tRNA/mir-34a Can Be Efficiently Biosynthesized in a Common Strain of *E. coli* on a Large Scale and Rapidly Purified to a High Degree of Homogeneity. To achieve high-yield production of pre–miR-34a agents in *E. coli*, we chose to use the tRNA scaffold (Ponchon and Dardel, 2007; Ponchon et al., 2009) to assemble a fusion ncRNA namely tRNA/mir-34a (Fig. 1A). The secondary structures predicted by different computational algorithms all indicated that the stem-loop structure of pre–miR-34a consisting of Dicer cleavage sites would be retained within tRNA/mir-34a chimeras. Thus the pre–miR-34a coding sequences were cloned to offer tRNA/mir-34a expression plasmids. Our data showed that slight change in the length of pre–miR-34a did not alter the levels of recombinant tRNA/mir-34a accumulated (Supplemental Fig. 1A). Target tRNA/mir-34a agents were expressed in different *E. coli* strains, and the highest accumulation levels were found in HST08 cells (Fig. 1B) at 9–14 hours post-transformation (Supplemental Fig. 1B). In addition, use of HST08-competent cells prepared within our laboratory offered similar levels of recombinant tRNA/mir-34a (Supplemental Fig. 1C), and the high-level expression (e.g., ~15% of recombinant ncRNAs in total RNAs) was retained when bacterial cultures were scaled up to 0.5 liters, and different batches of cultures were carried out (Supplemental Fig. 1D), demonstrating a consistent and efficient expression of biologic tRNA/mir-34a agents.

Next, we aimed to purify the recombinant tRNA/mir-34a to a high degree of homogeneity (e.g., >98%). Affinity purification was originally carried out for tRNA/mir-34a and the control tRNA/MSA bearing a Sephadex aptamer tag. Although affinity chromatography offered a good purity (>90%), overall yield was not very satisfactory (around 2% of recombinant ncRNA/total RNAs), which may be attributed to an unexpected but obvious inefficient binding (Supplemental Fig. 1E). Thus, we developed an anion-exchange FPLC method for the isolation of tRNA/mir-34a and tRNA/MSA from total RNAs using a salt gradient elution. This FPLC method not only enabled rapid isolation of target ncRNAs (<25 minutes per run; Fig. 1C) to a high degree of homogeneity (e.g., >98% purity, as demonstrated by gel electrophoresis, not shown) and HPLC analysis (Fig. 1D) but

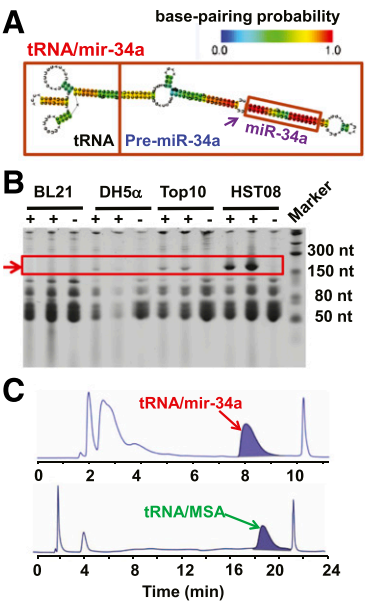

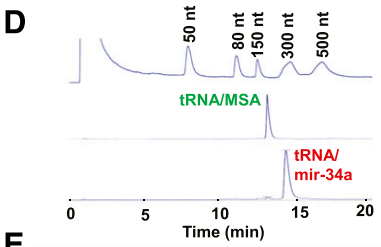

E

Oligo-Nucleotide	m/z (Da/e)	Location in tRNA/MSA	Location in tRNA/mir-34a
CUACG	763.1	C3:G7	C3:G7
[s4U]AG	933.1	[s4U]8:G10	[s4U]8:G10
CUCAG	763.1	C11:G15	C11:G15
CUCA[Gm]UUG	1248.7	C11:G18	C11:G18
[D][D]AG	613.4	[D]20:G23	[D]20:G23
CAG	916.2	C26:G28	C26:G28
UAAUUUACG	1398.7	U37:G45	U37:G45
[m7G][acp3U]CACAG	1157.7	[m7G]77:G83	[m7G]:G203
[m5U]ψCG	1213.1	[m5U]85:G88	[m5U]211:G214
AAUCCCG	1080.1	A89:G95	A215:G221
CCACCA	907.5	C102:A107	C228:A233
UUUCUUUG	1211.1		U73:G80
CAAUCAG	1092.1		C121:G127
UAUACUG	1081.4		U132:G138
CCCAAG	927.3		C165:G170

Fig. 1. Production and structural characterization of recombinant tRNA/mir-34a agents. (A) The secondary structure of chimeric tRNA/mir-34a (233 nt) predicted by CentroidFold showed that the stem-loop structure of mir-34a persisted within the chimeric ncRNA. The heat color gradation indicates the base-pairing probability from 0 to 1. (B) Expression of tRNA/mir-34a in various strains of *E. coli*. Among those tested, the highest levels of recombinant ncRNAs were found in HST08. (C) FPLC traces of tRNA/mir-34a and tRNA/MSA during the purification. Total RNAs were separated using anion-exchange FPLC and monitored at 260 nm. (D) HPLC analysis confirmed the high homogeneity (>98%) of purified tRNA/mir-34a and tRNA/MSA. (E) Liquid chromatography–tandem mass spectroscopy mapping/sequencing of purified tRNA/mir-34a and tRNA/MSA after the digestion with RNase T1. All post-transcriptional modifications except deoxyadenosine identified by nucleoside analysis (Supplemental Fig. 1) could be mapped to RNase T1 digestion products and assigned to specific sites.

also offered much higher purification yield (e.g., 67% according to the 15% target ncRNA present in total RNAs, or 10% recombinant ncRNA/total RNAs loaded on column). This FPLC method largely facilitated the purification process that allows us to readily obtain milligrams of ncRNAs, i.e., ~1.5 mg of >98% pure tRNA/mir-34a from 15 mg of total RNAs isolated from 0.5 liters of bacterial culture at all times.

Recombinant ncRNAs Carry Post-Transcriptional Modifications. To delineate if the recombinant tRNA/mir-34a comprise any post-transcriptional modifications, which are common for natural RNAs produced in living cells (Novoa et al., 2012), we employed several mass spectrometry–based techniques to analyze the purified ncRNAs after confirming their primary sequences by Sanger sequencing of reversely transcribed cDNAs (data not shown). First, we determined the molecular weights through electrospray ionization mass spectrometry analyses of the intact ncRNAs, which were 73,422.4 Da for tRNA/mir-34a and 34,765.2 Da for tRNA/MSA. The differences between the measured and predicted molecular weights (146.8 Da for tRNA/mir-34a and 149.2 Da for tRNA/MSA; Supplemental Fig. 2A) suggest the presence of modified nucleosides. We then conducted a liquid chromatography–UV and mass spectrometry detection analysis of ncRNA hydrolysates and identified a number of modified nucleosides for the tRNA scaffold (existing in both tRNA/mir-34a and tRNA/MSA), such as dihydrouridine (D), pseudouridine (ψ), 7-methylguanosine (m^7G), 4-thiouridine (s^4U), 2′-*O*-methylguanosine (Gm), and 3-(3-amino-3-carboxypropyl)uridine (acp^3U) (Supplemental Fig. 2B). We thus carried out liquid chromatography–tandem mass spectroscopy analyses (Supplemental Fig. 2C) of RNA fragments produced from recombinant ncRNAs by RNase T1, which allowed us to successfully map the ncRNA sequences and localize all modified nucleosides for the tRNA scaffold (Fig. 1E). The deoxyadenosine (dA) found in tRNA/mir-34a hydrolysates (Supplemental Fig. 2B) was not mapped to its RNase T1 digestions, which might be attributable to prior carryover or copurified nucleic acid. Together, these data indicate that recombinant ncRNAs obtained from *E. coli* indeed consist of various post-transcriptional modifications that may be critical for RNA folding and metabolic stability.

tRNA-Carried Pre–miR-34a Is Selectively Processed to Mature miR-34a in Human Carcinoma Cells, Whereas the tRNA Scaffold Is Degraded to tRNA Fragments. To assess whether chimeric tRNA/mir-34a can be selectively processed to mature miR-34a in human cells, we first conducted unbiased deep-sequencing study. The RNAseq data revealed that the tRNA/mir-34a chimera was precisely processed to mature miR-34a in A549 cells, leading to a 70-fold increase in miR-34a levels compared to cells treated with tRNA/MSA or vehicle (Fig. 2, A and B). In contrast, there was no or limited changes in other cellular miRNAs, except a few undefined small RNAs (e.g., hsa-miR-30c-5p_R+1 and hsa-mir-7641-1-p5_1ss6TC, etc.; Fig. 2, A and B; Supplemental Tables 1 and 2), which might be secondary effects that were caused by the changes in miR-34a target gene expression (see the results below). Furthermore, the increase in miR-34a levels was attributed to the 22- and 23-nt isoforms that arose in tRNA/mir-34a–, tRNA/MSA-, and vehicle-treated cells (Supplemental Table 3). In addition, the common tRNA scaffold was degraded in the cells to offer the same tRFs that exhibited similar patterns between tRNA/mir-34a– and tRNA/MSA-treated cells, but at much lower levels than mature miR-34a (Fig. 2B; Supplemental Table 4), supporting the use of tRNA/MSA as a proper control to distinguish the activities of pre–miR-34a.

Recombinant tRNA/mir-34a Exhibits a Favorable Cellular Stability and Is Degradable by Human RNases. Consistent with deep-sequencing data, selective stem-loop reverse transcription qRT-PCR analyses revealed a 70- to 100-fold increase in mature miR-34a levels in human lung (A549 and H460) and liver (HepG2 and Huh-7) carcinoma cells after the transfection with tRNA/mir-34a (Fig. 3A). Moreover, mature miR-34a and pre–miR-34a levels were elevated in tRNA/mir-34a–treated A549 cells in a dose-dependent manner, whereas there was no change of miR-34a levels in cells treated with tRNA/MSA, even though tRNA/MSA levels actually increased (Fig. 3B). Most importantly,

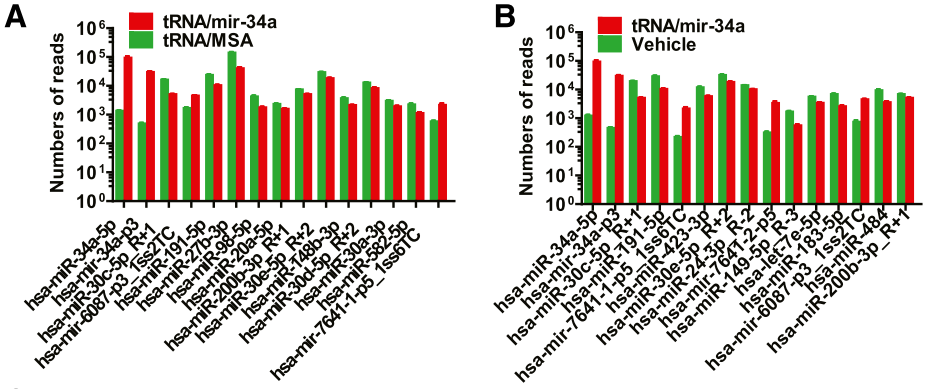

Fig. 2. The tRNA-carried pre–miR-34a was selectively processed to mature miR-34a in human carcinoma cells while tRNA scaffold was degraded to tRFs, as revealed by unbiased deep sequencing studies. Mature miR-34a levels were over 70-fold higher in A549 cells treated with 5 nM tRNA/mir-34a, compared with cells treated with the control tRNA/MSA (A) or vehicle (B). This was associated with a 60- to 65-fold increase in the numbers of reads of 15-nt miR-34a-p3 fragment (5′-CACGUUGUGGGGCCC-3′). In contrast, changes in other miRNAs were small or insignificant (Supplemental Tables 1 and 2), except for several undefined small RNAs (e.g., hsa-mir-7641-1-p5_1ss6TC). Values are mean ± S.D. of triplicate treatments that were sequenced separately. (C) Mapping major tRFs derived from tRNA/mir-34a and tRNA/MSA in A549 cells. Other low-abundance tRFs are provided in Supplemental Table 4.

a high level of recombinant tRNA/mir-34a and tRNA/MSA persisted for 6 days in the cells post-transfection with levels gradually decreasing from day 3 (Fig. 3C), indicating a favorable cellular stability. In addition, the change of pre–miR-34a and mature miR-34a levels over time were solely dependent on the tRNA/mir-34a treatment. Further biochemical experiments demonstrated that tRNA/mir-34a and tRNA/MSA were readily processed by RNase A (or RNase I, the major form of ribonuclease in human serum) and Dicer (RNase III) but to a relatively lower degree by angiogenin (RNase 5) (Fig. 3D), suggesting their involvement in the processing and degradation of recombinant ncRNAs. In contrast, bacterial RNase R was unable to cleave chimeric ncRNAs (data not shown), providing a good explanation

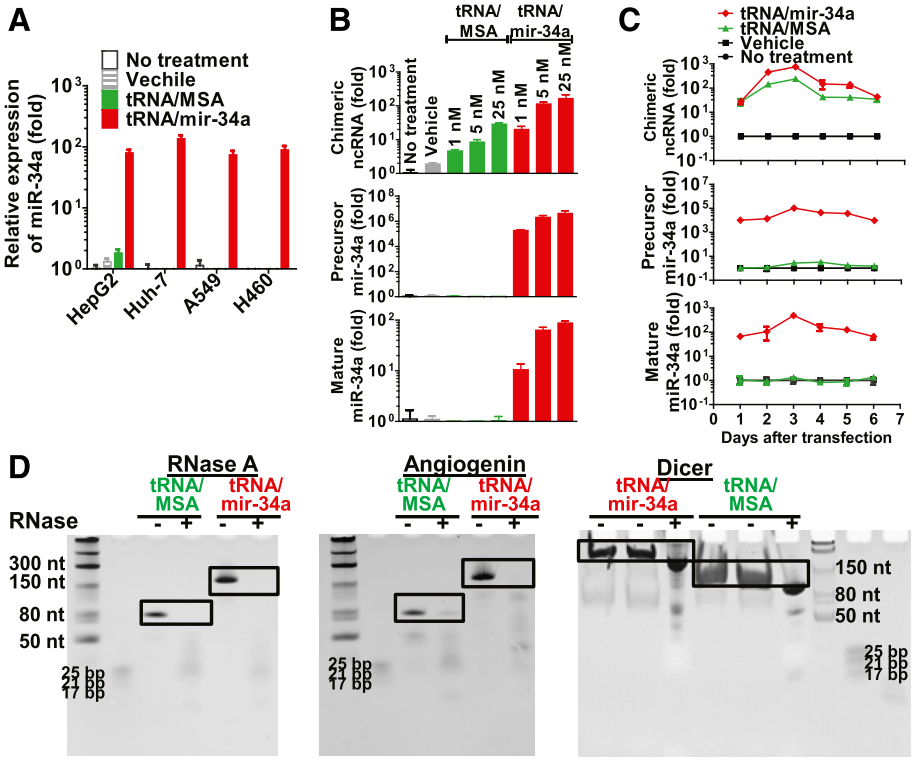

Fig. 3. Cellular stability and RNase susceptibility of chimeric tRNA/mir-34a. (A) Chimeric tRNA/mir-34a was processed to mature miR-34a in various types of human carcinoma cells, as determined by selective stem-loop reverse transcription qRT-PCR analyses. Values are mean ± S.D. of triplicate treatments. (B) The levels of chimeric ncRNA (tRNA/mir-34a or tRNA/MSA), pre-miRNA mir-34a, and mature miRNA miR-34a were increased in a dose-dependent manner ($P < 0.001$, one-way analysis of variance) in A549 cells at 24 hours after transfection with 1, 5, or 25 nM of FPLC-purified tRNA/mir-34a or tRNA/MSA. Note that mir-34a and miR-34a levels were only elevated in cells treated with tRNA/mir-34a. (C) Chimeric ncRNA (tRNA/mir-34a or tRNA/MSA; 5 nM) exhibited good stability in A549 cells. Note that change in mature miR-34a levels was dependent on tRNA/mir-34a treatment. (D) Chimeric tRNA/mir-34a and the tRNA/MSA were susceptible to a number of human RNases, including RNase A, angiogenin, and Dicer. RNase digestions were analyzed with 8% urea-PAGE.

for why such ncRNAs were accumulated to high levels within bacteria.

tRNA-Carried Pre–miR-34a Is Active in Reducing miR-34a Target Gene Expression and Inhibiting Cancer Cell Proliferation, Equally or More Effectively Than Synthetic miR-34a Agents. We thus assessed the efficacy of tRNA-carried pre–miR-34a in the control of miR-34a target gene expression and cancer cell growth, using tRNA/MSA as a critical control. Recombinant tRNA/mir-34a showed a dose-dependent inhibition against the proliferation of all types of cancer cells tested in our studies, to a much greater degree than the control tRNA/MSA (Fig. 4A; Supplemental Fig. 3). The higher efficacy in suppressing cancer cell growth by tRNA/mir-34a was also indicated by the estimated EC_{50} values (Table 1). Inhibition of A549 and HepG2 carcinoma cell proliferation by tRNA/mir-34a was associated with a remarkable repression of a number of well defined miR-34a target genes such as CDK6, SIRT1, and MET, compared with the tRNA/MSA or vehicle treatments (Fig. 4B). In addition, we compared side-by-side the effectiveness of biologic and synthetic miR-34a agents in human cell line models. Interestingly, our data showed that recombinant tRNA/mir-34a was relatively more effective in suppressing the proliferation of A549 and HepG2 cells and the protein levels of miR-34a target genes (e.g., CDK6, SIRT1, and MET) than the same doses of synthetic pre–miR-34a and miR-34a mimics bearing artificial modifications, compared with corresponding controls (Fig. 5, A and B). These results indicate that tRNA-carried pre–miR-34a is biologically/pharmacologically active in the modulation of miR-34a target gene expression and cancer cell proliferation.

Recombinant Pre–miR-34a Is Effective in Suppressing Xenograft Tumor Progression in Mouse Models. We thus evaluated the therapeutic effects of tRNA/mir-34a in vivo using human lung carcinoma A549 and hepatic carcinoma HepG2 xenograft tumor mouse models. When A549 xenograft tumors reached ~150 mm^3, typically within 3 weeks of inoculation, we treated male nude mice intratumorally with 20 or 100 μg of in vivo–jetPEI-formulated tRNA/mir-34a, which would not be complicated by tissue distribution. Separate groups of animals were administered the same doses of in vivo–jetPEI-formulated tRNA/MSA or only the in vivo–jetPEI vehicle as controls. Our data showed that, compared with the vehicle treatment or the same dose of tRNA/MSA, the higher dose (100 μg) of tRNA/mir-34a led to a complete disappearance of the A549 xenograft tumors (three out of six) and an overall significant repression of the outgrowth of viable tumors (Fig. 6A). The same dose (100 μg) of tRNA/mir-34a also significantly suppressed the growth of HepG2-derived xenografts (Fig. 6B), although to a lesser degree than its effects on A549 xenografts. These findings indicate that recombinant tRNA-carried pre–miR-34a is effective in controlling xenograft tumor progression in vivo.

Chimeric ncRNAs Are Well Tolerated in Mouse Models. We further investigated the safety profiles of recombinant tRNA/mir-34a agents produced in *E. coli*. The LAL assay was first conducted to evaluate whether these biologic ncRNAs contain significant levels of endotoxin that may cause immune response or toxicity in mammalian cells. While total RNAs isolated from *E. coli* showed variable levels of endotoxin (100–1000 EU/μg of RNA), endotoxin activities were minimal for the ncRNAs purified with FPLC (<10 EU/μg of RNA) and those further processed with an endotoxin removal kit (<3.0 EU/μg of RNA). Despite the lack of an endotoxin safety standard for RNA agents and the uncertainty of whether RNAs influence (the mechanism of) the LAL assay, endotoxin activities in our purified ncRNAs measured much lower than 2000 EU/μg of DNA that is required to significantly inhibit transfection and cell proliferation (Butash et al., 2000).

After verifying that in vivo–jetPEI-loaded tRNA/mir-34a and tRNA/MSA were protected against degradation by serum

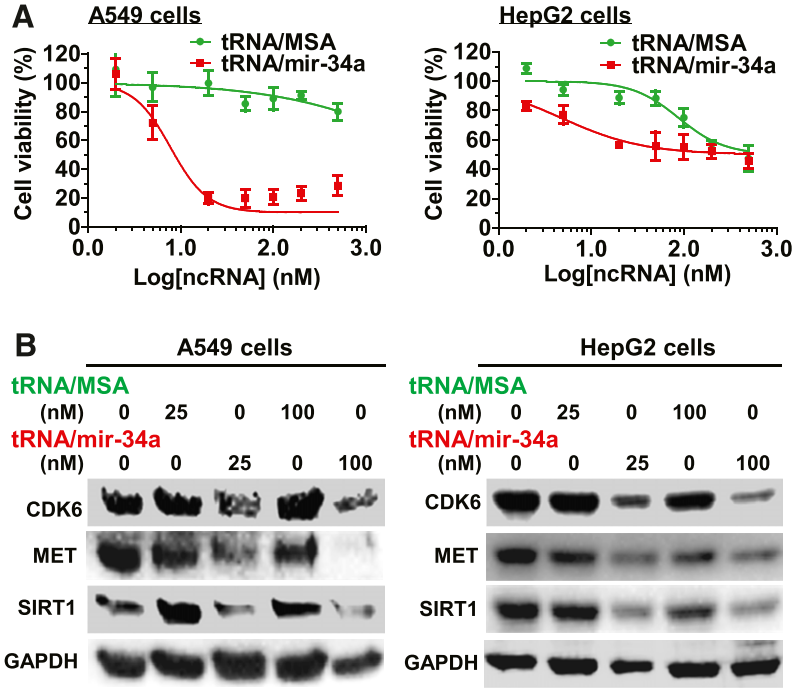

Fig. 4. Recombinant mir-34a was biologically/pharmacologically active in suppressing cancer cell proliferation and target gene expression. (A) tRNA/mir-34a inhibited the growth of human carcinoma A549 and HepG2 cells in a dose-dependent manner and to a much greater degree than the control tRNA/MSA ($P < 0.001$, two-way analysis of variance). Antiproliferative activities against H460 and Huh-7 cells are shown in Supplemental Fig. 3, and the estimated ED_{50} and Hill slope values are provided in Table 1. Cell viability was determined using MTT [3-(4,5-dimethylthiazol-2-yl)-2,5-diphenyltetrazolium bromide] assay at 72 hour post-transfection. Values are mean ± S.D. of triplicate cultures. (B) Compared with the control tRNA/MSA, recombinant tRNA/mir-34a sharply reduced the protein levels of a number of miR-34a target genes including CDK6, MET, and SIRT1 in A549 and HepG2 cells. Western blots were conducted using protein-selective antibodies. GAPDH was used as a loading control.

TABLE 1
Estimated EC_{50} and Hill slope values for the suppression of human carcinoma cell proliferation by recombinant tRNA/mir-34a and control tRNA/MSA

Cell Lines	EC_{50}		Hill Slope	
	tRNA/MSA	tRNA/mir-34a	tRNA/MSA	tRNA/mir-34a
	nM			
A549	Not fitted	7.80 ± 1.19	Not fitted	−2.18 ± 0.59
H460	158 ± 1	5.72 ± 1.09*	−0.86 ± 0.20	−1.32 ± 0.14*
HepG2	87.9 ± 1.1	4.75 ± 1.21*	−1.74 ± 0.40	−0.96 ± 0.18*
Huh-7	Not fitted	11.1 ± 1.2	Not fitted	−0.66 ± 0.07

Goodness of fit, $R^2 > 0.75$. Not fitted, goodness of fit is less than 0.50.
*$P < 0.05$, significantly different from the control tRNA/MSA in the same cell line.

RNases (Fig. 7A), we directly assessed the effects of in vivo–jetPEI-formulated ncRNAs on the immune response as well as hepatic and renal functions in immunocompetent BALB/c male mouse models. The activation of immune response is often indicated by the increase of blood levels of various cytokines, among which the pro- and anti-inflammatory cytokine IL-6 is the most sensitive in response to nucleic acids (Wiggins et al., 2010). As a positive control, LPS-treated mice showed an immediate sharp surge of serum IL-6 levels 1–6 hour after injection (Fig. 7B), in addition to obvious signs of stress (e.g., hunched posture and labored movement), and then fully recovered within 24 hours. In contrast, serum IL-6 levels were just elevated slightly in mice 6 hours after intravenous administration of 100 μg tRNA/mir-34a or tRNA/MSA. The change was very mild compared with the LPS treatment and it was similar to that reported for synthetic miR-34a mimics (Wiggins et al., 2010), which might not indicate an adverse drug response. Furthermore, mouse blood chemistry profiles, including the levels of alanine aminotransferase, aspartate aminotransferase, albumin, alkaline phosphatase, total bilirubin, blood urea nitrogen, creatinine, and total protein were not significantly altered by recombinant tRNA/mir-34a (Fig. 7C), suggesting that the biologic ncRNA agents did not induce acute liver or kidney toxicity.

Discussion

In contrast to the great efforts to develop miRNA-based therapies, translational and clinical research is often hampered by a lack of access to large quantities of inexpensive natural miRNA agents. Motivated by the concept of deploying biologic RNA agents to perform RNA actions and the principle of "prodrug," we established a novel strategy to cost effectively produce multimilligrams of tRNA fusion miR-34a biologic agents in 1-liter cultures of a common strain of *E. coli* in a research laboratory setting. The better expression of recombinant ncRNA in HST08 strain may be related to the lack of gene clusters in HST08 cells for digesting methylated DNA or a lower capacity to polyadenylate ncRNA for degradation. Notably, our strategy is different from a newly reported approach of generating fully-processed small interfering RNAs using p19-expressing bacteria (Huang et al., 2013). A high-yield accumulation of recombinant tRNA/mir-34a in bacteria (~15% of total RNAs) also facilitated the purification by anion-exchange FPLC method to a high degree of homogeneity (>98%). In addition, we were able to characterize the primary structures and modified nucleosides of recombinant ncRNAs through liquid chromatography–UV and mass spectrometry detection analyses of hydrolysates and liquid chromatography–tandem mass spectroscopy analyses of RNase T1-cleaved fragments. Our findings illustrate fundamental post-transcriptional modifications of the tRNA

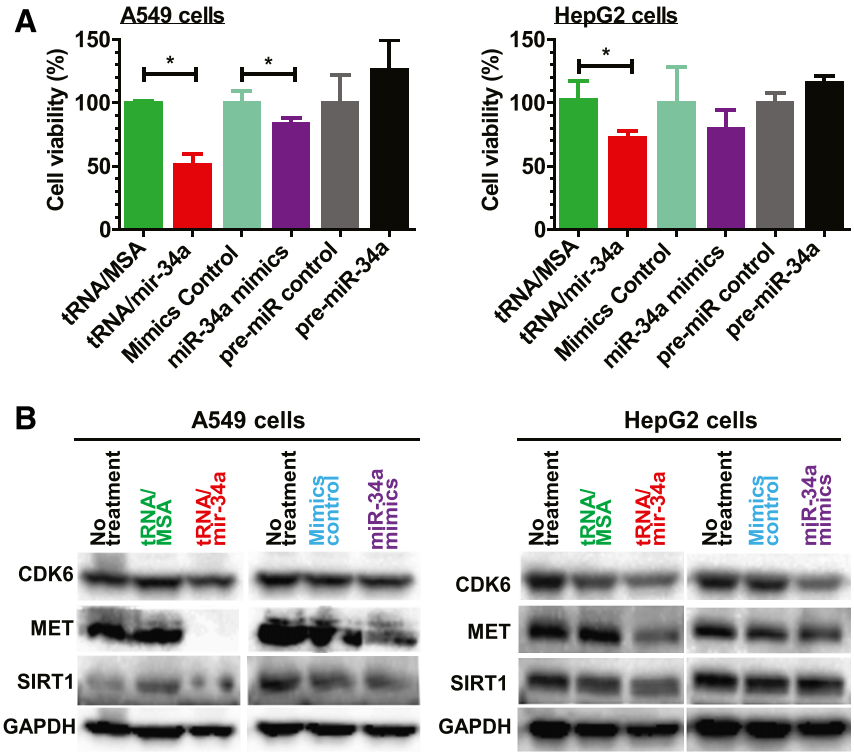

Fig. 5. Recombinant mir-34a was equally or more effective than synthetic miR-34a mimics in reducing human carcinoma cell proliferation and target gene expression. (A) The effects of 5 nM biologic tRNA/mir-34a, and synthetic miR-34a precursor and mimics on the growth of A549 and HepG2 carcinoma cells. Cell viability was determined using MTT [3-(4,5-dimethylthiazol-2-yl)-2,5-diphenyltetrazolium bromide] assay at 72 hours post-transfection. Values are mean ± S.D. of triplicate treatments. *$P < 0.05$, compared with corresponding control. (B) The effects of 25 nM recombinant mir-34a and synthetic miR-34a mimics on the protein levels of miR-34a target genes CDK6, MET, and SIRT1 in A549 and HepG2 carcinoma cells, as determined by Western blots at 72 hours post-transfection.

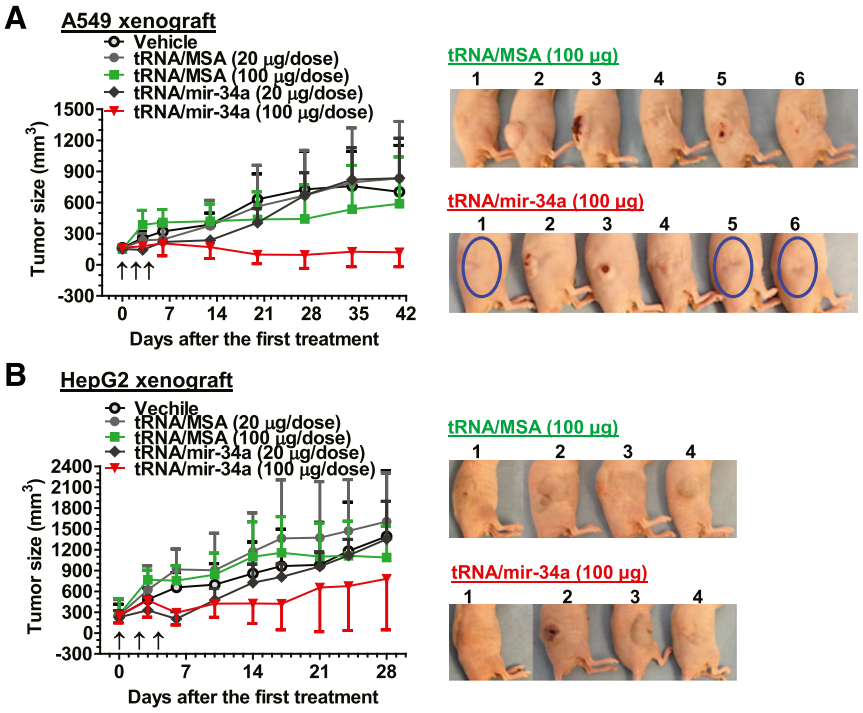

Fig. 6. Recombinant mir-34a was effective in controlling xenograft tumor progression in mouse models. (A) Compared with the same dose of tRNA/MSA or vehicle control, tRNA/mir-34a (100 μg) significantly ($P < 0.001$, unpaired t test) suppressed the growth of A549 xenograft tumors. Note that the tumors in three mice completely disappeared after the treatment with 100 μg of tRNA/mir-34a. (B) Growth of HepG2 xenograft tumors were also significantly ($P < 0.01$, unpaired t test) suppressed by the 100-μg dose tRNA/mir-34a treatment, compared with the same dose of tRNA/MSA or vehicle. FPLC-purified ncRNAs were administered intratumorally every the other day for three times. Values are mean ± S.D. ($N = 6$ per group for A549 xenografts; $N = 4$ per group for HepG2 xenografts). Separate groups of mice ($N = 4$) were treated with vehicle as additional controls.

scaffold that are critical for its stability (Alexandrov et al., 2006).

Chimeric tRNA/mir-34a showed a rather surprisingly favorable stability within human carcinoma cells, suggesting that the tRNA carrier also offered a "stealth delivery" of target pre–miR-34a into human cells beyond the high-yield production of chimeric tRNA/mir-34a in bacteria. As expected, chimeric tRNA/mir-34a acted as a prodrug in human carcinoma cells, where pre–miR-34a was selectively processed to mature miR-34a by intrinsic miRNA processing machinery, and the tRNA carrier was degraded to tRFs (Lee et al., 2009; Li et al., 2012). The 70-fold higher levels of mature miR-34a were also accompanied by 60-fold increase in miR-34a-p3 small RNA derived from pre–miR-34a. Therefore, chimeric tRNA/mir-34a may serve as an optimal carrier to assemble small RNAs of interests (Chen et al., 2015) that cannot be produced with tRNA scaffold. In addition, these results offer a good understanding of the fate of recombinant ncRNAs in human cells and the susceptibility to a few commercially-available human RNases, even though the precise contribution

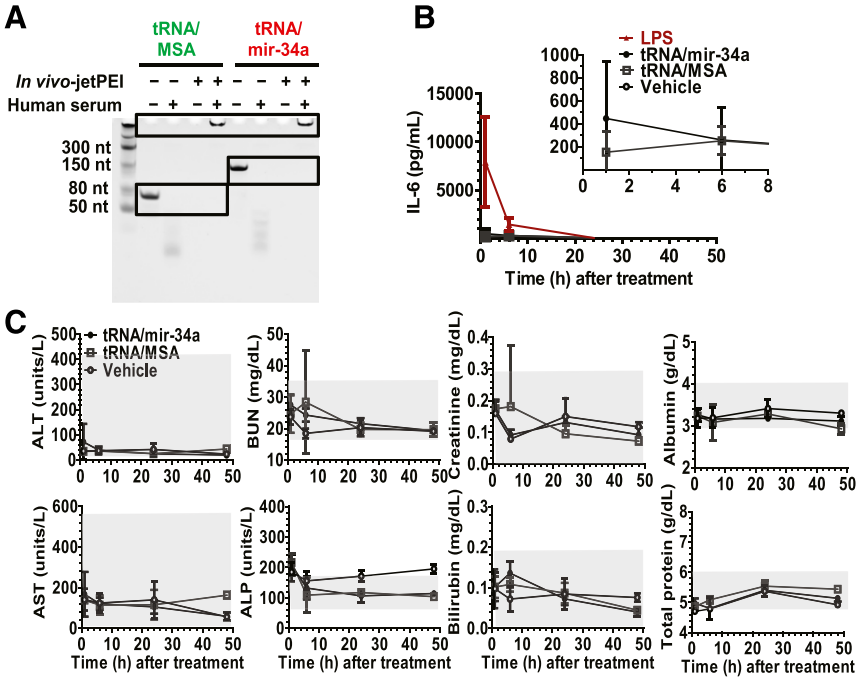

Fig. 7. Biologic ncRNAs were well tolerated in mouse models. (A) In vivo–jetPEI-loaded ncRNAs were protected against degradation by serum RNases. (B) Compared with vehicle control treatment, in vivo–jetPEI formulated recombinant ncRNAs (100 μg i.v.) did not cause significant change in mouse serum IL-6 levels whereas lipopolysaccharide did (two-way analysis of variance with Bonferroni post-tests). (C) Recombinant ncRNAs (100 μg i.v.) had no significant influence on blood chemistry profiles, including alanine aminotransferase (ALT), aspartate aminotransferase (AST), blood urea nitrogen (BUN), alkaline phosphatase (ALP), creatinine, total bilirubin, albumin, and total protein. The gray-shaded area indicates the guideline ranges reported by the Comparative Pathology Laboratory at UC-Davis. Values are mean ± S.D. ($N = 3$–4 mice per time point and treatment).

of specific RNases to the metabolism and pharmacokinetics of biologic tRNA/mir-34a warrants further investigation. While the effects of these tRFs are unknown, the same tRFs were produced from tRNA/MSA and tRNA/mir-34a at comparable levels in human cells, supporting the validity of using tRNA/MSA expressed in the same strain of *E. coli* and purified in the same manner as a control for the assessment of bioactivities of tRNA-carried pre–miR-34a.

The functions of tRNA-carried pre–miR-34a were nicely demonstrated by the selective reduction of protein expression levels of a number of previously verified miR-34a target genes, such as CDK6, MET, and SIRT1, in both A549 and HepG2 cells, compared with tRNA/MSA. These genes are critical for many cellular processes such as cell cycle and apoptosis. Therefore, the suppression of miR-34a target genes by recombinant pre–miR-34a provides a mechanistic explanation for its antiproliferative activities. The broad anticancer activities of recombinant pre–miR-34a against various types of cancer cells are consistent with previous findings on miR-34a functions in targeting multiple oncogenes and oncogenic pathways among different types of cancer cells (Chang et al., 2007; He et al., 2007; Sun et al., 2008; Yamakuchi et al., 2008; Li et al., 2009; Liu et al., 2011; Kasinski and Slack, 2012). Meanwhile, different human carcinoma cell lines did exhibit variable sensitivities to tRNA/mir-34a, which may be attributable to the variability in genome and gene expression profiles as well as the apparent effects of pre–miR-34a on target gene expression in different cell lines. While we posit that the activities of tRNA-carried pre–miR-34a in the modulation of miR-34a target gene expression and cancer cell growth is attributable to the mature miR-34a selectively produced from chimeric tRNA/mir-34a, we cannot exclude the possibility that pre–miR-34a itself is responsible for some of the effects noted.

Non–small-cell lung cancer A549 cells containing Kirsten rat sarcoma viral oncogene homolog (*KRAS*) mutation, wild-type p53, and wild-type epidermal growth factor receptor, commonly found in human lung carcinomas, are proper models for human lung carcinogenesis and tumor progression (Lehman et al., 1991; Nomoto et al., 2006). By contrast, the hepatocellular carcinoma HepG2 cell line represents a pure human liver carcinoma cell line free of viral infections, comprises an NRAS mutation, and is often used as an hepatocellular carcinoma model (Hsu et al., 1993; Charette et al., 2010; Costantini et al., 2013). Therefore, the A549 and HepG2 cells were used to produce xenograft tumors in mouse models to evaluate the effectiveness of recombinant pre–miR-34a in the control of tumor growth in vivo. Our study revealed a significant suppression of both A549 and HepG2 xenograft tumor growth by the higher dose (100 μg) of tRNA/mir-34a, compared with the vehicle treatment or the same dose of tRNA/MSA. After monitoring tumor growth for 6 weeks, we demonstrated that tRNA/mir-34a strikingly eradicated A549 tumors (three out of six mice), although it is unknown whether and when recurrence would occur. Although we did not measure the half-life of tRNA/mir-34a in vivo, we observed that expression levels persisted until day 6 in A549 and HepG2 cell lines after single-dose transfection. Meanwhile, we showed a much greater degree of inhibition against A549 xenografts than HepG2 by tRNA/mir-34a, which is in agreement with the efficacy of tRNA/mir-34a defined with cancer cell line models in vitro. While this study is limited to an intratumoral drug administration, it provides direct evidence to support the effectiveness of biologic miR-34a agents in vivo. Nevertheless, the utility of recombinant miR-34a agents for cancer treatments should be challenged by using targeted drug delivery systems and/or more clinically relevant tumor animal models before clinical investigations.

Our study also illustrated that a relatively higher dose intravenous bolus, FPLC-purified chimeric miR-34a biologic agents, did not cause any stress to the mice (e.g., hunched posture and labored movement) within 48 hours after drug administration or alter the liver and kidney functions as manifested by the unchanged blood chemistry profiles. The levels of serum IL-6, the most sensitive cytokine in response to nucleic acids, were only slightly perturbed by chimeric ncRNAs compared with LPS treatment. The minor change in IL-6 levels caused by recombinant tRNA/mir-34 and tRNA/MSA within a short period (6 hours) was actually comparable to those reported for synthetic miR-34a mimics (Wiggins et al., 2010). Owing to unchanged levels of alanine aminotransferase, aspartate aminotransferase, bilirubin, albumin, blood urea nitrogen, creatinine, and total proteins in tRNA/mir-34a-treated mice 48 hours postinjection, these findings indicate that recombinant ncRNAs are well tolerated in mouse models and do not induce acute toxicity. Nevertheless, further studies are needed to critically define the safety profiles following chronic administration of biologic ncRNAs in different species of animal models before clinical studies.

It is also noteworthy that recombinant tRNA/mir-34a, as first described in the current study, was proven to be equally or more effective than synthetic pre–miR-34a and miR-34a mimics in the regulation of target gene expression and suppression of cancer cell proliferation, compared with corresponding controls. This might be related to the differences in their secondary structures and metabolic stabilities within the cells, and consequently the efficiencies of miRNA processing machinery and RNA-induced silencing complex in utilizing these agents for the regulation of target gene expression and control of cellular processes. Nevertheless, the advantages and disadvantages of using recombinant miRNA agents versus synthetic miRNAs, as well as recombinant DNAs for research and therapy, will be undoubtedly subjected to discussion and examination.

In conclusion, our results demonstrated that chimeric pre–miR-34a agents could be efficiently produced in a common strain of *E. coli* on a large scale. The biologic tRNA/mir-34a bearing natural modifications exhibited a favorable cellular stability and was degradable by RNases. Furthermore, tRNA-carried pre–miR-34a was pharmacologically active in suppressing human carcinoma cell proliferation through the regulation of miR-34a target gene expression after being selectively processed to mature miR-34a. In addition, chimeric miR-34a was effective in controlling xenograft tumor progression and it was well tolerated in mouse models. Our findings indicate that chimeric miRNA agents engineered in bacteria may be useful tools for the discovery and development of novel pharmacotherapies.

Authorship Contributions

Participated in research design: Yu, Wang, Ho, Chen, Addepalli, Limbach, M.-M. Li, Wu, Jilek, Qiu, Zhang, T. Li, Wun, White, Lam.

Conducted experiments: Wang, Ho, Chen, Addepalli, M.-M. Li, Wu, Jilek, Yu, Qiu.

Contributed new reagents or analytic tools: Yu, Limbach, Li, Addepalli, Lam.

Performed data analysis: Wang, Ho, Chen, Addepalli, Limbach, M.-M. Li, Wu, Jilek, Qiu, Zhang, T. Li, Wun, White, Lam, Yu.

Wrote or contributed to the writing of the manuscript: Yu, Wang, Ho, Chen, Addepalli, Limbach, M.-M. Li, Wu, Jilek, Qiu, Zhang, T. Li, Wun, White, Lam.

References

Alexandrov A, Chernyakov I, Gu W, Hiley SL, Hughes TR, Grayhack EJ, and Phizicky EM (2006) Rapid tRNA decay can result from lack of nonessential modifications. *Mol Cell* **21**:87–96.

Bader AG (2012) miR-34 - a microRNA replacement therapy is headed to the clinic. *Front Genet* **3**:120.

Bi HC, Pan YZ, Qiu JX, Krausz KW, Li F, Johnson CH, Jiang CT, Gonzalez FJ, and Yu AM (2014) N-methylnicotinamide and nicotinamide N-methyltransferase are associated with microRNA-1291-altered pancreatic carcinoma cell metabolome and suppressed tumorigenesis. *Carcinogenesis* **35**:2264–2272.

Bodeman CE, Dzierlenga AL, Tally CM, Mulligan RM, Lake AD, Cherrington NJ, and McKarns SC (2013) Differential regulation of hepatic organic cation transporter 1, organic anion-transporting polypeptide 1a4, bile-salt export pump, and multidrug resistance-associated protein 2 transporter expression in lymphocyte-deficient mice associates with interleukin-6 production. *J Pharmacol Exp Ther* **347**:136–144.

Butash KA, Natarajan P, Young A, and Fox DK (2000) Reexamination of the effect of endotoxin on cell proliferation and transfection efficiency. *Biotechniques* **29**: 610–614, 616, 618–619.

Chang TC, Wentzel EA, Kent OA, Ramachandran K, Mullendore M, Lee KH, Feldmann G, Yamakuchi M, Ferlito M, Lowenstein CJ, et al. (2007) Transactivation of miR-34a by p53 broadly influences gene expression and promotes apoptosis. *Mol Cell* **26**:745–752.

Charette N, De Saeger C, Lannoy V, Horsmans Y, Leclercq I, and Stärkel P (2010) Salirasib inhibits the growth of hepatocarcinoma cell lines in vitro and tumor growth in vivo through ras and mTOR inhibition. *Mol Cancer* **9**:256.

Chen QX, Wang WP, Zeng S, Urayama S, and Yu AM (2015) A general approach to high-yield biosynthesis of chimeric RNAs bearing various types of functional small RNAs for broad applications. *Nucleic Acids Res* **43**:3857–3869.

Costantini S, Di Bernardo G, Cammarota M, Castello G, and Colonna G (2013) Gene expression signature of human HepG2 cell line. *Gene* **518**:335–345.

Craig VJ, Tzankov A, Flori M, Schmid CA, Bader AG, and Müller A (2012) Systemic microRNA-34a delivery induces apoptosis and abrogates growth of diffuse large B-cell lymphoma in vivo. *Leukemia* **26**:2421–2424.

He L, He X, Lim LP, de Stanchina E, Xuan Z, Liang Y, Xue W, Zender L, Magnus J, Ridzon D, et al. (2007) A microRNA component of the p53 tumour suppressor network. *Nature* **447**:1130–1134.

Hsu IC, Tokiwa T, Bennett W, Metcalf RA, Welsh JA, Sun T, and Harris CC (1993) p53 gene mutation and integrated hepatitis B viral DNA sequences in human liver cancer cell lines. *Carcinogenesis* **14**:987–992.

Huang L, Jin J, Deighan P, Kiner E, McReynolds L, and Lieberman J (2013) Efficient and specific gene knockdown by small interfering RNAs produced in bacteria. *Nat Biotechnol* **31**:350–356.

Ingelman-Sundberg M, Zhong XB, Hankinson O, Beedanagari S, Yu AM, Peng L, and Osawa Y (2013) Potential role of epigenetic mechanisms in the regulation of drug metabolism and transport. *Drug Metab Dispos* **41**:1725–1731.

Kasinski AL and Slack FJ (2011) Epigenetics and genetics. MicroRNAs en route to the clinic: progress in validating and targeting microRNAs for cancer therapy. *Nat Rev Cancer* **11**:849–864.

Kasinski AL and Slack FJ (2012) miRNA-34 prevents cancer initiation and progression in a therapeutically resistant K-ras and p53-induced mouse model of lung adenocarcinoma. *Cancer Res* **72**:5576–5587.

Kelnar K, Peltier HJ, Leatherbury N, Stoudemire J, and Bader AG (2014) Quantification of therapeutic miRNA mimics in whole blood from nonhuman primates. *Anal Chem* **86**:1534–1542.

Krivos KL, Addepalli B, and Limbach PA (2011) Removal of 3′-phosphate group by bacterial alkaline phosphatase improves oligonucleotide sequence coverage of RNase digestion products analyzed by collision-induced dissociation mass spectrometry. *Rapid Commun Mass Spectrom* **25**:3609–3616.

Lee YS, Shibata Y, Malhotra A, and Dutta A (2009) A novel class of small RNAs: tRNA-derived RNA fragments (tRFs). *Genes Dev* **23**:2639–2649.

Lehman TA, Bennett WP, Metcalf RA, Welsh JA, Ecker J, Modali RV, Ullrich S, Romano JW, Appella E, Testa JR, et al. (1991) p53 mutations, ras mutations, and p53-heat shock 70 protein complexes in human lung carcinoma cell lines. *Cancer Res* **51**:4090–4096.

Li MM, Addepalli B, Tu MJ, Chen QX, Wang WP, Limbach PA, LaSalle J, Zeng S, Huang M, and Yu AM (2015) Chimeric miR-1291 biosynthesized efficiently in E. coli is effective to reduce target gene expression in human carcinoma cells and improve chemosensitivity. *Drug Metab Dispos* DOI:115.064493 [published ahead of print].

Li MM, Wang WP, Wu WJ, Huang M, and Yu AM (2014) Rapid production of novel pre-microRNA agent hsa-mir-27b in Escherichia coli using recombinant RNA technology for functional studies in mammalian cells. *Drug Metab Dispos* **42**: 1791–1795.

Li Y, Guessous F, Zhang Y, Dipierro C, Kefas B, Johnson E, Marcinkiewicz L, Jiang J, Yang Y, Schmittgen TD, et al. (2009) MicroRNA-34a inhibits glioblastoma growth by targeting multiple oncogenes. *Cancer Res* **69**:7569–7576.

Li Z, Ender C, Meister G, Moore PS, Chang Y, and John B (2012) Extensive terminal and asymmetric processing of small RNAs from rRNAs, snoRNAs, snRNAs, and tRNAs. *Nucleic Acids Res* **40**:6787–6799.

Liu C, Kelnar K, Liu B, Chen X, Calhoun-Davis T, Li H, Patrawala L, Yan H, Jeter C, Honorio S, et al. (2011) The microRNA miR-34a inhibits prostate cancer stem cells and metastasis by directly repressing CD44. *Nat Med* **17**:211–215.

Ma L, Teruya-Feldstein J, and Weinberg RA (2007) Tumour invasion and metastasis initiated by microRNA-10b in breast cancer. *Nature* **449**:682–688.

Nelissen FH, Leunissen EH, van de Laar L, Tessari M, Heus HA, and Wijmenga SS (2012) Fast production of homogeneous recombinant RNA—towards large-scale production of RNA. *Nucleic Acids Res* **40**:e102.

Nomoto K, Tsuta K, Takano T, Fukui T, Fukui T, Yokozawa K, Sakamoto H, Yoshida T, Maeshima AM, Shibata T, et al. (2006) Detection of EGFR mutations in archived cytologic specimens of non-small cell lung cancer using high-resolution melting analysis. *Am J Clin Pathol* **126**:608–615.

Novoa EM, Pavon-Eternod M, Pan T, and Ribas de Pouplana L (2012) A role for tRNA modifications in genome structure and codon usage. *Cell* **149**:202–213.

Pan YZ, Zhou A, Hu Z, and Yu AM (2013) Small nucleolar RNA-derived microRNA hsa-miR-1291 modulates cellular drug disposition through direct targeting of ABC transporter ABCC1. *Drug Metab Dispos* **41**:1744–1751.

Ponchon L, Beauvais G, Nonin-Lecomte S, and Dardel F (2009) A generic protocol for the expression and purification of recombinant RNA in Escherichia coli using a tRNA scaffold. *Nat Protoc* **4**:947–959.

Ponchon L and Dardel F (2007) Recombinant RNA technology: the tRNA scaffold. *Nat Methods* **4**:571–576.

Pramanik D, Campbell NR, Karikari C, Chivukula R, Kent OA, Mendell JT, and Maitra A (2011) Restitution of tumor suppressor microRNAs using a systemic nanovector inhibits pancreatic cancer growth in mice. *Mol Cancer Ther* **10**: 1470–1480.

Russell SP and Limbach PA (2013) Evaluating the reproducibility of quantifying modified nucleosides from ribonucleic acids by LC-UV-MS. *J Chromatogr B Analyt Technol Biomed Life Sci* **923-924**:74–82.

Sun F, Fu H, Liu Q, Tie Y, Zhu J, Xing R, Sun Z, and Zheng X (2008) Downregulation of CCND1 and CDK6 by miR-34a induces cell cycle arrest. *FEBS Lett* **582**: 1564–1568.

Taucher M and Breuker K (2010) Top-down mass spectrometry for sequencing of larger (up to 61 nt) RNA by CAD and EDD. *J Am Soc Mass Spectrom* **21**:918–929.

Wang Y, Shan X, Dai Y, Jiang L, Chen G, Zhang Y, Wang Z, Dong L, Wu J, Guo G, et al. (2015) Curcumin analog L48H37 prevents lipopolysaccaride-induced TLR4 signaling pathway activation and sepsis via targeting MD2. *J Pharmacol Exp Ther* **352**:539–550.

Welch C, Chen Y, and Stallings RL (2007) MicroRNA-34a functions as a potential tumor suppressor by inducing apoptosis in neuroblastoma cells. *Oncogene* **26**: 5017–5022.

Wiggins JF, Ruffino L, Kelnar K, Omotola M, Patrawala L, Brown D, and Bader AG (2010) Development of a lung cancer therapeutic based on the tumor suppressor microRNA-34. *Cancer Res* **70**:5923–5930.

Yamakuchi M, Ferlito M, and Lowenstein CJ (2008) miR-34a repression of SIRT1 regulates apoptosis. *Proc Natl Acad Sci USA* **105**:13421–13426.

Yao HW and Li J (2015) Epigenetic modifications in fibrotic diseases: implications for pathogenesis and pharmacological targets. *J Pharmacol Exp Ther* **352**:2–13.

Yu AM (2009) Role of microRNAs in the regulation of drug metabolism and disposition. *Expert Opin Drug Metab Toxicol* **5**:1513–1528.

Address correspondence to: Dr. Ai-Ming Yu, Department of Biochemistry and Molecular Medicine, UC Davis School of Medicine, 2700 Stockton Blvd., Suite 2132, Sacramento, CA. E-mail: aimyu@ucdavis.edu

Bioengineering novel chimeric microRNA-34a for prodrug cancer therapy: High-yield expression and purification, and structural and functional characterization

Wei-Peng Wang, Pui Yan Ho, Qiu-Xia Chen, Balasubrahmanyam Addepalli, Patrick A. Limbach, Mei-Mei Li, Wen-Juan Wu, Joseph L. Jilek, Jing-Xin Qiu, Hong-Jian Zhang, Tianhong Li, Theodore Wun, Ralph DeVere White, Kit S. Lam, Ai-Ming Yu

LIST OF SUPPLEMENTARY MATERIALS

Supplementary Figure S1. Expression and affinity purification of recombinant tRNA/mir-34a. (A) tRNA/mir-34a-129nt (233 nt in total) and tRNA/mir-34a-112nt (216 nt in total) chimeras were expressed at comparably high levels in HST08 *E. coli*. The tRNA/mir-34a-129nt was chosen for further investigation which is simply named tRNA/mir-34a. (B) Time course of tRNA/mir-34a levels accumulated within HST08 cells after transformation indicated that higher ncRNA levels were achieved at 9-14 hr post-transformation. Chimeric tRNA/mir-34a levels were determined by qPCR assay, normalized to bacterial 16S, and then multiplied by the quantities of total RNAs isolated from corresponding cultures. Values are mean ± SD of triplicate cultures. (C) Expression/accumulation levels of tRNA/mir-34a using home-made and commercial HST08 competent cells were comparable. (D) Consistent high-level expression of recombinant ncRNAs in different batches of 0.5 L bacterial cultures. (E) Urea-PAGE analysis of RNA fractions during affinity purification using Sephadex G-100 beads. While pure recombinant ncRNAs were readily obtained, the overall purification yields were very low (e.g., ~2% recombinant ncRNAs/total RNAs) due to an obvious poor binding to the Sephadex aptamer.

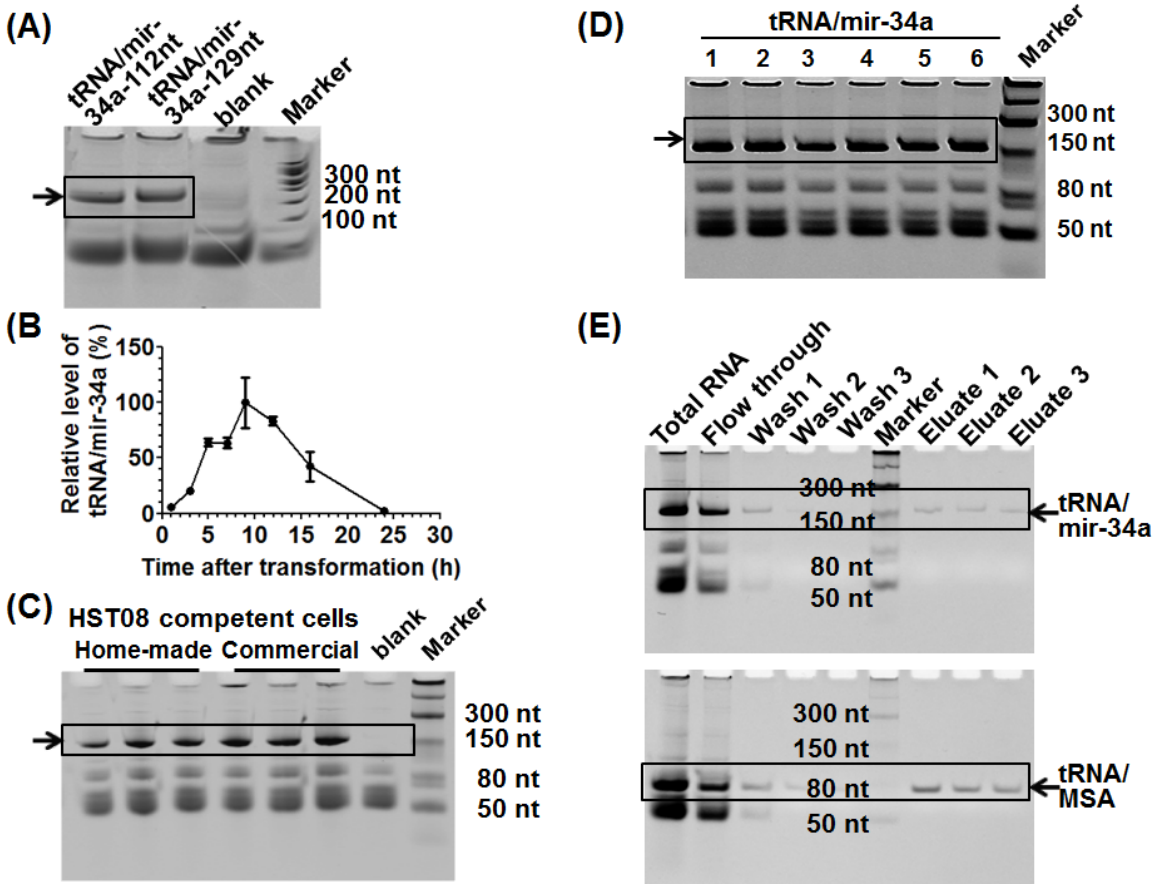

Supplementary Figure S2. Structural characterization of recombinant tRNA/mir-34a and tRNA/MSA purified by anion-exchange FPLC. (A) The molecular weight (MW) of intact ncRNA was determined by electrospray ionization mass spectrometry (ESI-MS) analyses, followed by deconvolution of multiply protonated ions. The differences between the measured and predicted MWs of tRNA/mir-34a and tRNA/MSA suggest the presence of posttranscriptionally modified nucleosides. (B) Identification of posttranscriptionally modified nucleosides through LC-UV-MS analyses of the hydrolysates of recombinant ncRNAs. Shown are LC-UV traces of the hydrolysates of tRNA/MSA and tRNA/mir-34a, and individual peaks were assigned to natural nucleosides based on their retention times and mass spectra. D, dihydrouridine; ψ, pseudouridine; C, cytidine; acp^{3}U, 3-(3-amino-3-carboxypropyl)uridine; U, uridine; m^{5}U, 5-methyluridine; G, guanosine; m^{7}G, 7-methylguanosine; S^{4}U, 4-thiouridine; Gm, 2'-*O*-methylguanosine; m^{1}G, 1-methylguanosine; A, adenosine; dA, deoxyadenosine. (C) RNase T1 mapping tRNA/mir-34a and tRNA/MSA. Shown are the total ion LC-MS chromatograms of RNase T1-digested tRNA/MSA and tRNA/mir-34a, and the identification of an example fragment [m^{7}G][acp^{3}U]CACAG (m/z 1157.76, [M-2H$^+$]$^{2-}$) eluted at 33.0 min based upon the MS/MS fragment ions.

(A)

ncRNA	Sequence (5'→3')	Predicted MW (Da)	Measured MW (Da)
tRNA/mir-34a	GGCUACGUAGCUCAGUUGGUUAGAGCAGCGGCCGAGUAAUUUACGUCGACGUGG ACCGGCCAGCUGUGAGUGUUUCUUUGGCAGUGUCUUAGCUGGUUGUUGUGAGCA AUAGUAAGGAAGCAAUCAGCAAGUAUACUGCCCUAGAAGUGCUGCACGUUGUGG GGCCCAAGAGGGAAGAUGACGUCGAUGGUUGCGGCCGCGGGUCACAGGUUCGAA UCCCGUCGUAGCCACCA	75463.2	75610.0
tRNA/MSA	GGCUACGUAGCUCAGUUGGUUAGAGCAGCGGCCGAGUAAUUUACGUCGACGGUG ACGUCGAUGGUUGCGGCCGCGGGUCACAGGUUCGAAUCCCGUCGUAGCCACCA	34616.0	34765.2

(B)

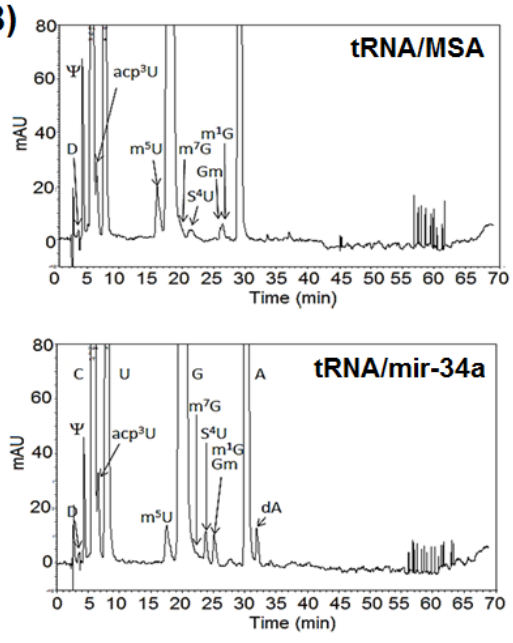

(C)

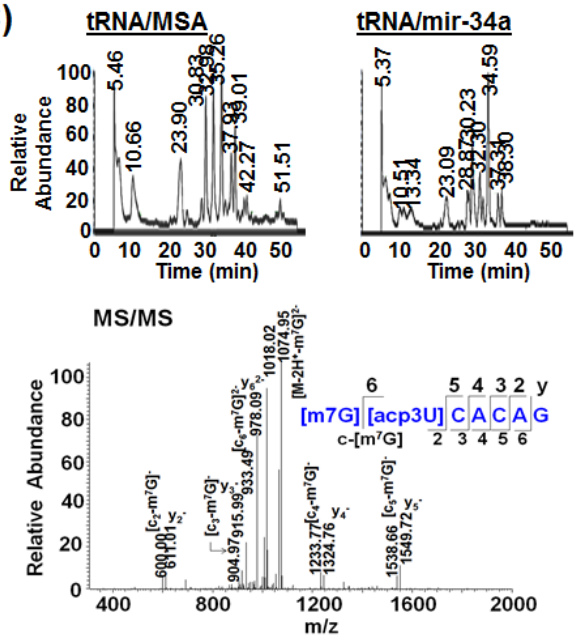

Supplementary Figure S3. Recombinant tRNA/mir-34a inhibited the growth of lung H460 (A) and liver Huh-7 (B) human carcinoma cells in a dose dependent manner and to greater degree than the control tRNA/MSA (*P* < 0.001, two-way ANOVA). Cells transfected with the same doses of tRNA/MSA were used as controls. Cell viability was determined using MTT assay at 72 h post-transfection. Values are mean ± SD of triplicate treatments.

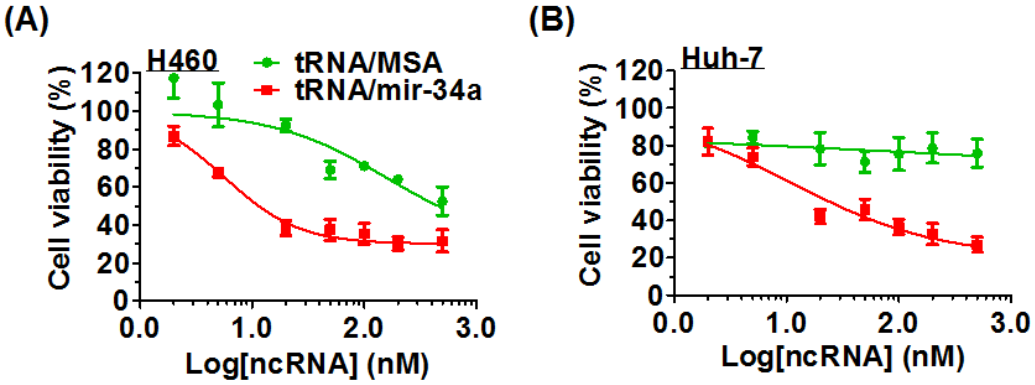

Supplementary Table S1. Change in miRNA levels in A549 cells after the treatment with tRNA/mir-34a, as compared with tRNA/MSA. The numbers of reads of individual miRNAs were determined by deep sequencing analysis of small RNAs isolated from the cells at 48 h post-transfection. Each group consisted of triplicate treatments that were sequenced separately.

Index	Reporter Name	p-value	tRNA/mir-34a over tRNA/MSA Ratio	tRNA/MSA Mean	tRNA/MSA StDev	tRNA/mir-34a Mean	tRNA/mir-34a StDev	MSA-1 # Reads	MSA-2 # Reads	MSA-3 # Reads	34a-1 # Reads	34a-2 # Reads	34a-3 # Reads
10	hsa-mir-34a-p3	4.26E-06	60.7	467	43	28,342	3,508	444	440	516	31,220	24,435	29,372
45	hsa-miR-30c-5p_R+1	1.23E-05	0.3	15,541	853	4,829	242	16,193	14,576	15,856	4,758	4,631	5,099
9	hsa-mir-6087-p3_1ss2TC	7.85E-05	2.7	1,600	121	4,322	295	1,607	1,716	1,475	4,317	4,619	4,029
74	hsa-miR-191-5p	1.13E-04	0.4	22,618	1,550	9,999	573	22,512	21,124	24,218	9,357	10,180	10,459
38	**hsa-miR-34a-5p**	1.63E-04	69.0	1,292	84	89,095	16,937	1,212	1,285	1,379	108,629	80,164	78,492
51	hsa-miR-27b-3p	3.73E-04	0.3	134,559	12,009	38,530	5,135	141,030	120,702	141,945	38,465	43,698	33,428
14	hsa-miR-98-5p	4.61E-04	0.4	4,058	413	1,692	166	4,401	3,600	4,174	1,699	1,855	1,524
67	hsa-miR-20a-5p	7.46E-04	0.7	2,212	113	1,513	73	2,308	2,087	2,239	1,597	1,463	1,478
68	hsa-miR-200b-3p_R+1	1.06E-03	0.7	7,057	392	4,867	234	7,387	6,624	7,159	4,675	5,127	4,798
43	hsa-miR-30e-5p_R+2	1.10E-03	0.6	28,023	1,655	17,383	1,285	28,725	26,132	29,211	18,821	16,981	16,347
86	hsa-miR-148b-3p	1.22E-03	0.6	3,512	286	2,028	114	3,531	3,217	3,789	2,157	1,941	1,986
44	hsa-miR-30d-5p_R+2	2.62E-03	0.6	12,172	893	7,893	650	12,865	11,164	12,488	8,538	7,902	7,238
48	hsa-miR-30a-3p	2.63E-03	0.6	2,866	225	1,835	152	3,105	2,658	2,836	1,953	1,889	1,663
21	hsa-miR-582-5p	2.67E-03	0.5	2,148	249	1,078	145	1,927	2,099	2,418	1,065	941	1,229
7	hsa-mir-7641-1-p5_1ss6TC	2.73E-03	3.8	551	51	2,071	419	527	610	517	2,022	2,513	1,679
54	hsa-miR-26a-5p	4.05E-03	0.6	24,889	1,211	14,497	1,454	25,398	23,507	25,762	13,009	15,914	14,567
103	hsa-let-7e-5p	4.13E-03	0.6	5,368	597	3,260	261	6,045	4,916	5,144	3,183	3,551	3,046
5	hsa-mir-7641-2-p5	4.62E-03	3.9	816	90	3,216	747	898	830	719	3,563	3,727	2,359
46	hsa-miR-30b-5p	5.35E-03	0.7	5,159	284	3,361	315	4,873	5,163	5,441	3,433	3,016	3,634
76	hsa-miR-183-5p	6.44E-03	0.5	5,190	173	2,478	300	5,018	5,363	5,187	2,132	2,658	2,645
24	hsa-miR-4792_1ss9GT	7.18E-03	4.3	350	32	1,513	430	338	386	327	1,995	1,376	1,168
20	hsa-miR-7-5p_R+1	8.18E-03	0.7	1,683	109	1,250	30	1,807	1,637	1,604	1,278	1,219	1,253
52	hsa-miR-27a-3p	8.72E-03	0.6	27,713	1,939	17,110	2,123	25,677	27,927	29,537	14,927	17,233	19,169

Following miRNAs shown significant difference but have the number of reads < the average (1496) of the data set.

740	hsa-miR-335-3p	1.15E-05	0.3	546	8	150	5	537	549	553	145	154	150
653	hsa-miR-4443_L+1R-2	2.93E-05	10.9	39	4	427	58	36	38	44	494	394	393
974	hsa-let-7f-1-3p_1ss22CT	3.35E-05	0.2	146	11	32	3	151	133	153	36	31	30
531	hsa-miR-582-3p	4.67E-05	0.3	711	30	188	13	709	682	742	199	174	191
573	hsa-miR-543_R-1	9.74E-05	2.4	89	5	209	14	92	91	83	197	206	225
816	hsa-miR-222-5p_L+2R-2	1.19E-04	0.2	228	19	50	2	241	238	206	52	50	47
804	hsa-miR-25-5p_R+2	1.27E-04	0.4	150	10	61	5	155	138	157	62	66	57
829	hsa-miR-203a-3p_L-1R+1	1.59E-04	7.9	21	3	162	32	21	24	17	198	138	150
711	hsa-miR-363-3p	2.31E-04	2.7	17	1	46	4	16	18	16	46	42	50
382	hsa-mir-4449-p5_1ss13GC	2.33E-04	5.7	6	1	37	6	7	7	6	44	34	33
453	hsa-miR-941	2.50E-04	0.3	660	50	224	23	688	603	691	237	238	197
545	hsa-miR-561-5p	2.56E-04	0.2	284	16	63	1	289	266	297	64	62	64
559	hsa-miR-548k	3.37E-04	0.2	318	44	72	12	351	268	336	83	74	60
924	hsa-miR-128-3p	4.10E-04	0.5	673	39	327	9	714	637	668	317	334	329
639	hsa-miR-4488_L-2R-1	4.21E-04	3.6	54	7	194	28	58	46	57	205	216	162
847	hsa-miR-1910-5p	5.33E-04	0.4	57	2	25	2	57	56	60	26	26	23
838	hsa-miR-197-3p	5.67E-04	0.5	359	29	189	13	390	354	332	198	196	174
634	hsa-miR-4516_L-3R+1	6.66E-04	4.7	128	26	605	88	107	158	119	704	580	533
406	hsa-mir-3656-p3_1ss13AC	7.03E-04	4.0	21	3	86	16	17	22	24	103	82	71
730	hsa-miR-342-3p_R+1	7.03E-04	0.7	689	23	451	5	682	714	670	445	452	456
796	hsa-miR-296-3p_L-1R+1	8.30E-04	0.4	103	6	36	4	96	107	107	37	40	32
611	hsa-miR-4787-5p_L-1R-5_1ss5GC	9.10E-04	3.9	9	2	36	7	7	10	11	42	37	29
339	hsa-mir-641-p3	1.27E-03	0.4	71	6	32	4	65	78	70	36	32	28
449	hsa-miR-98-3p_1ss22CT	1.38E-03	0.3	101	5	35	4	96	99	107	31	39	35
338	hsa-mir-663a-p3_1ss11CA	1.61E-03	3.0	45	6	134	9	39	47	50	129	129	143
975	hsa-let-7e-3p	1.62E-03	0.4	57	4	24	3	56	54	61	26	21	26
978	hsa-let-7b-3p_1ss22CT	1.67E-03	0.3	281	22	94	15	267	269	306	89	83	111
973	hsa-let-7f-2-3p_1ss22CT	1.69E-03	0.2	39	4	10	2	38	36	44	12	8	9
480	hsa-miR-758-3p_1ss22CT	1.74E-03	0.3	234	22	63	11	223	220	259	64	51	74
757	hsa-miR-3195_R-2	1.78E-03	3.8	53	11	199	22	47	66	46	224	181	191

696	hsa-miR-374a-3p	1.78E-03	0.5	524	39	286	9	483	528	561	287	295	277
719	hsa-miR-361-5p	1.95E-03	0.6	601	32	363	30	567	607	631	376	328	384
627	hsa-miR-455-3p_R+1	2.00E-03	0.5	254	25	121	5	280	231	251	127	118	119
631	hsa-miR-4521_R+4	2.02E-03	0.4	854	80	380	54	797	820	945	337	363	441
867	hsa-miR-181a-2-3p	2.08E-03	0.5	243	25	112	16	265	216	247	129	108	98
564	hsa-miR-548av-3p_L+2	2.38E-03	0.2	37	4	7	2	32	39	39	6	5	8
777	hsa-miR-30e-3p	2.42E-03	0.5	925	114	479	51	1,046	819	911	510	506	420
476	hsa-miR-7704_1ss19GC	2.52E-03	3.7	59	6	219	43	62	52	61	256	230	172
505	hsa-miR-654-3p_R-2	2.52E-03	0.2	1,009	65	230	45	984	960	1,083	280	213	196
497	hsa-miR-665_R-2	2.53E-03	0.5	539	72	255	34	467	540	610	216	271	278
445	hsa-mir-1248-p5_1ss14CA	2.53E-03	3.1	24	5	77	12	19	30	24	69	71	91
325	hsa-mir-7108-p3_1ss16GT	2.67E-03	3.1	33	3	103	18	30	35	35	124	88	99
888	hsa-miR-141-3p_R-1	2.69E-03	1.8	49	5	89	5	43	51	53	93	90	83
909	hsa-miR-1303_L+1	2.87E-03	0.5	192	24	87	14	203	165	209	80	104	78
669	hsa-miR-409-3p	3.04E-03	0.5	784	20	382	34	806	771	774	348	417	381
322	hsa-mir-7641-1-p3	3.06E-03	3.3	53	13	177	38	68	50	42	148	220	163
942	hsa-miR-1260b_R-1	3.16E-03	0.6	171	17	105	9	159	190	163	115	97	103
911	hsa-miR-1296-5p_R-2	3.34E-03	0.2	400	8	82	14	397	394	409	96	69	83
592	hsa-miR-500a-3p_R+1	3.42E-03	0.4	344	45	139	26	385	351	296	114	167	136
778	hsa-miR-30d-3p	3.61E-03	0.4	174	32	64	14	160	152	211	79	62	52
481	hsa-miR-744-5p_R-1	3.67E-03	0.6	876	39	493	48	896	832	901	530	510	439
26	hsa-miR-450b-5p_R-1	4.10E-03	0.4	1,282	98	467	85	1,346	1,169	1,332	391	559	451
733	hsa-miR-33b-3p_R-1	4.22E-03	0.2	105	5	20	4	101	103	110	25	16	19
85	hsa-miR-149-5p_R-3	4.41E-03	0.4	1,356	84	531	81	1,449	1,330	1,288	440	554	598
808	hsa-miR-23b-5p_L-1	4.69E-03	0.3	270	46	86	20	323	250	237	63	99	96
902	hsa-miR-132-3p	4.74E-03	1.6	41	2	66	6	41	44	39	71	67	59
908	hsa-miR-1304-3p_1ss13CA	4.78E-03	0.5	207	35	99	14	247	179	197	106	109	84
979	hsa-let-7a-3p_R+1	4.84E-03	0.5	445	21	208	26	466	424	444	179	217	228
724	hsa-miR-34c-5p	5.50E-03	0.4	224	21	98	17	242	201	227	112	103	79
457	hsa-miR-93-3p_R+1	5.88E-03	0.3	63	4	22	4	67	58	63	23	17	25
717	hsa-miR-3614-5p_R-1	6.56E-03	4.2	9	1	36	9	8	9	9	34	45	27

496	hsa-miR-671-3p	6.95E-03	0.4	144	24	54	12	162	116	153	60	61	39
853	hsa-miR-18a-5p_R+1	7.57E-03	0.6	241	20	155	18	219	254	251	173	137	156
685	hsa-miR-378c_R-5	7.85E-03	2.3	24	1	55	9	22	24	24	65	53	47
471	hsa-miR-7977_L-1_1ss6AG	7.91E-03	1.5	253	8	374	31	249	262	248	387	339	396
731	hsa-miR-340-5p	8.02E-03	0.6	839	111	487	71	803	750	963	568	436	458
6	hsa-mir-7641-2-p3	8.53E-03	3.1	319	18	997	202	317	337	302	1,158	1,063	771
682	hsa-miR-379-3p_R-1	8.60E-03	0.6	34	5	19	3	29	37	36	18	17	23
677	hsa-miR-3909	8.67E-03	0.2	82	8	14	4	89	84	73	18	16	9
663	hsa-miR-424-3p_R+1	8.76E-03	2.5	233	18	588	124	252	216	231	731	501	533
556	hsa-miR-548s_R-1	8.85E-03	0.4	45	11	17	5	58	41	37	13	16	22
817	hsa-miR-22-5p_R-1	8.89E-03	1.7	98	3	165	18	94	100	100	156	152	186
925	hsa-miR-128-1-5p	9.27E-03	0.5	41	8	21	4	40	34	50	20	25	18
695	hsa-miR-374b-3p	9.70E-03	0.5	90	7	43	8	89	98	84	38	52	38
522	hsa-miR-6126_L-2R-1_1ss16AG	9.91E-03	5.4	56	12	303	139	52	70	46	462	236	210
550	hsa-miR-550a-5p_R-1	9.93E-03	0.4	103	4	40	7	104	98	106	32	43	45
635	hsa-miR-4508_L+2	9.93E-03	5.7	43	13	243	17	47	53	28	228	260	240

Supplementary Table S2. Change in miRNA levels in A549 cells after the treatment with tRNA/mir-34a, as compared with vehicle (Lipofectamine 2000). The numbers of reads of individual miRNAs were determined by deep sequencing analysis of small RNAs isolated from A549 cells at 48 h post-treatment. Each group consisted of triplicate treatments that were sequenced separately.

			tRNA/mir-34a over tRNA/MSA	**Vehicle**		**tRNA/mir-34a**		V1	V2	V3	34a-1	34a-2	34a-3
Index	Reporter Name	p-value	**Ratio**	**Mean**	**StDev**	**Mean**	**StDev**	# Reads	# Reads	# Reads	# Reads	# Reads	# Reads
10	hsa-mir-34a-p3	2.38E-06	65.3	434	47	28,342	3,508	421	486	396	31,220	24,435	29,372
45	hsa-miR-30c-5p_R+1	7.23E-06	0.3	18,515	1,050	4,829	242	18,035	19,719	17,790	4,758	4,631	5,099
38	hsa-miR-34a-5p	2.55E-05	76.6	1,164	128	89,095	16,937	1,110	1,310	1,071	108,629	80,164	78,492
74	hsa-miR-191-5p	1.38E-04	0.4	27,417	2,297	9,999	573	29,979	26,728	25,543	9,357	10,180	10,459
7	hsa-mir-7641-1-p5_1ss6TC	1.78E-04	10.0	208	29	2,071	419	232	215	176	2,022	2,513	1,679
32	hsa-miR-423-3p	5.97E-04	0.5	11,278	1,053	5,512	411	12,411	11,095	10,329	5,735	5,763	5,038
43	hsa-miR-30e-5p_R+2	6.54E-04	0.6	30,539	1,602	17,383	1,285	28,715	31,184	31,719	18,821	16,981	16,347
56	hsa-miR-24-3p_R-2	7.49E-04	0.7	13,326	436	9,660	419	13,016	13,825	13,137	9,226	9,692	10,062
5	hsa-mir-7641-2-p5	1.08E-03	10.7	301	33	3,216	747	305	332	267	3,563	3,727	2,359
85	hsa-miR-149-5p_R-3	1.12E-03	0.3	1,612	160	531	81	1,716	1,692	1,427	440	554	598
103	hsa-let-7e-5p	1.30E-03	0.6	5,350	368	3,260	261	5,761	5,234	5,054	3,183	3,551	3,046
76	hsa-miR-183-5p	1.36E-03	0.4	6,557	417	2,478	300	6,492	7,002	6,177	2,132	2,658	2,645
9	hsa-mir-6087-p3_1ss2TC	1.38E-03	6.1	713	126	4,322	295	783	787	568	4,317	4,619	4,029
23	hsa-miR-484	1.39E-03	0.4	8,986	987	3,400	548	9,854	9,192	7,912	3,167	3,008	4,026
68	hsa-miR-200b-3p_R+1	1.40E-03	0.7	6,542	285	4,867	234	6,272	6,840	6,514	4,675	5,127	4,798
24	hsa-miR-4792_1ss9GT	1.42E-03	11.1	136	15	1,513	430	147	142	119	1,995	1,376	1,168
51	hsa-miR-27b-3p	1.55E-03	0.2	181,402	5,820	38,530	5,135	176,432	187,805	179,968	38,465	43,698	33,428
21	hsa-miR-582-5p	1.97E-03	0.5	2,314	293	1,078	145	2,063	2,636	2,241	1,065	941	1,229
46	hsa-miR-30b-5p	2.26E-03	0.6	5,692	512	3,361	315	5,205	6,227	5,643	3,433	3,016	3,634
14	hsa-miR-98-5p	2.40E-03	0.4	4,623	86	1,692	166	4,561	4,721	4,588	1,699	1,855	1,524
99	hsa-miR-100-5p	2.44E-03	0.3	64,569	12,092	21,959	4,103	63,886	52,833	76,988	17,237	24,652	23,990
39	hsa-miR-331-3p_R+1	2.59E-03	0.5	1,579	152	733	109	1,741	1,556	1,440	681	659	858
89	hsa-miR-140-3p_L-1R+2	2.61E-03	0.6	1,560	120	986	43	1,631	1,628	1,421	1,011	1,012	936
69	hsa-miR-200a-3p_R+1	2.95E-03	2.1	1,786	162	3,774	539	1,635	1,958	1,767	4,347	3,277	3,699
52	hsa-miR-27a-3p	3.17E-03	0.5	31,963	2,827	17,110	2,123	30,581	35,215	30,092	14,927	17,233	19,169

86	hsa-miR-148b-3p	3.37E-03	0.5	3,928	434	2,028	114	3,431	4,234	4,117	2,157	1,941	1,986
44	hsa-miR-30d-5p_R+2	3.46E-03	0.6	14,068	390	7,893	650	14,511	13,917	13,777	8,538	7,902	7,238
57	hsa-miR-23b-3p_R+3	5.25E-03	0.5	5,217	303	2,609	355	5,365	5,416	4,868	2,991	2,288	2,548
12	hsa-miR-99b-5p	5.38E-03	0.5	21,893	3,514	11,171	1,213	21,042	18,882	25,754	9,783	12,028	11,703
54	hsa-miR-26a-5p	5.53E-03	0.6	25,358	935	14,497	1,454	25,024	26,414	24,635	13,009	15,914	14,567
37	hsa-miR-365b-3p	6.50E-03	0.4	3,159	160	1,245	219	3,274	3,227	2,976	1,127	1,111	1,497
48	hsa-miR-30a-3p	6.70E-03	0.6	2,933	74	1,835	152	2,868	3,014	2,916	1,953	1,889	1,663
93	hsa-miR-125a-5p	6.81E-03	0.3	45,119	3,034	13,619	2,798	48,372	44,618	42,366	10,401	14,989	15,468
11	hsa-mir-27b-p5	8.44E-03	1.4	5,021	273	6,944	583	4,768	5,311	4,984	6,300	7,095	7,437
35	hsa-miR-378a-3p	8.63E-03	0.5	3,796	176	1,746	285	3,957	3,824	3,608	2,073	1,612	1,553
Following miRNAs shown significant difference but have the number of reads < the average (1496) of the data set.													
740	hsa-miR-335-3p	1.06E-06	0.3	596	21	150	5	575	616	598	145	154	150
816	hsa-miR-222-5p_L+2R-2	3.58E-06	0.2	210	10	50	2	200	221	208	52	50	47
974	hsa-let-7f-1-3p_1ss22CT	1.66E-05	0.2	192	16	32	3	206	196	175	36	31	30
531	hsa-miR-582-3p	3.91E-05	0.3	752	63	188	13	678	786	790	199	174	191
829	hsa-miR-203a-3p_L-1R+1	4.34E-05	20.5	8	1	162	32	9	9	6	198	138	150
924	hsa-miR-128-3p	8.27E-05	0.5	696	31	327	9	728	694	665	317	334	329
453	hsa-miR-941	8.67E-05	0.3	883	75	224	23	932	919	796	237	238	197
653	hsa-miR-4443_L+1R-2	1.45E-04	14.1	30	2	427	58	32	28	31	494	394	393
797	hsa-miR-28-5p_R-1	1.62E-04	1.2	422	8	514	8	418	431	417	510	510	523
911	hsa-miR-1296-5p_R-2	1.72E-04	0.2	495	68	82	14	549	516	418	96	69	83
639	hsa-miR-4488_L-2R-1	2.22E-04	6.5	30	6	194	28	36	29	25	205	216	162
733	hsa-miR-33b-3p_R-1	2.38E-04	0.1	257	34	20	4	289	260	222	25	16	19
573	hsa-miR-543_R-1	3.05E-04	2.8	76	8	209	14	69	84	75	197	206	225
322	hsa-mir-7641-1-p3	3.36E-04	6.4	28	5	177	38	34	24	25	148	220	163
559	hsa-miR-548k	3.46E-04	0.2	323	48	72	12	267	350	352	83	74	60
978	hsa-let-7b-3p_1ss22CT	3.69E-04	0.2	382	42	94	15	385	423	340	89	83	111
449	hsa-miR-98-3p_1ss22CT	3.93E-04	0.3	115	16	35	4	102	133	110	31	39	35
757	hsa-miR-3195_R-2	4.07E-04	7.2	28	5	199	22	34	23	26	224	181	191
6	hsa-mir-7641-2-p3	4.08E-04	7.4	135	19	997	202	147	145	114	1,158	1,063	771
476	hsa-miR-7704_1ss19GC	5.26E-04	7.5	29	3	219	43	31	32	26	256	230	172

975	hsa-let-7e-3p	6.27E-04	0.3	73	5	24	3	76	75	67	26	21	26
339	hsa-mir-641-p3	6.29E-04	0.4	85	10	32	4	87	95	74	36	32	28
909	hsa-miR-1303_L+1	6.64E-04	0.3	283	36	87	14	319	284	246	80	104	78
457	hsa-miR-93-3p_R+1	1.14E-03	0.3	84	11	22	4	95	84	73	23	17	25
545	hsa-miR-561-5p	1.33E-03	0.2	282	28	63	1	250	296	301	64	62	64
857	hsa-miR-185-5p	1.43E-03	0.6	752	36	483	34	752	716	789	478	451	519
973	hsa-let-7f-2-3p_1ss22CT	1.45E-03	0.2	41	5	10	2	36	45	42	12	8	9
622	hsa-miR-4662b_L-3R-4_1ss15GC	1.47E-03	2.8	38	6	104	14	32	37	44	92	119	101
481	hsa-miR-744-5p_R-1	1.50E-03	0.5	976	112	493	48	1,100	883	946	530	510	439
804	hsa-miR-25-5p_R+2	1.70E-03	0.4	138	17	61	5	152	119	143	62	66	57
867	hsa-miR-181a-2-3p	1.84E-03	0.4	275	21	112	16	281	293	251	129	108	98
522	hsa-miR-6126_L-2R-1_1ss16AG	2.19E-03	17.8	17	9	303	139	26	16	9	462	236	210
338	hsa-mir-663a-p3_1ss11CA	2.19E-03	6.8	20	4	134	9	25	18	16	129	129	143
863	hsa-miR-181c-3p_L-1R+1	2.31E-03	0.4	99	5	39	5	105	98	94	46	37	36
505	hsa-miR-654-3p_R-2	2.34E-03	0.2	1,131	66	230	45	1,067	1,199	1,125	280	213	196
812	hsa-miR-2277-5p_R-1	2.36E-03	0.5	38	4	18	3	43	38	34	16	21	17
404	hsa-mir-3665-p5_1ss14AG	2.38E-03	9.0	61	20	554	241	67	78	39	830	450	383
695	hsa-miR-374b-3p	2.41E-03	0.4	110	16	43	8	96	107	127	38	52	38
946	hsa-miR-125b-1-3p	2.47E-03	0.7	624	34	438	30	662	595	616	427	472	415
480	hsa-miR-758-3p_1ss22CT	2.59E-03	0.2	261	17	63	11	260	278	244	64	51	74
94	hsa-miR-1246_R+1	2.68E-03	5.5	27	5	148	4	32	25	24	150	144	151
817	hsa-miR-22-5p_R-1	2.72E-03	1.8	94	7	165	18	102	87	93	156	152	186
677	hsa-miR-3909	2.81E-03	0.1	99	19	14	4	117	101	79	18	16	9
631	hsa-miR-4521_R+4	2.86E-03	0.5	829	130	380	54	749	759	979	337	363	441
853	hsa-miR-18a-5p_R+1	3.01E-03	0.6	277	23	155	18	272	303	257	173	137	156
778	hsa-miR-30d-3p	3.02E-03	0.3	212	23	64	14	222	228	185	79	62	52
796	hsa-miR-296-3p_L-1R+1	3.05E-03	0.3	113	22	36	4	129	121	88	37	40	32
550	hsa-miR-550a-5p_R-1	3.08E-03	0.3	115	11	40	7	121	123	103	32	43	45
838	hsa-miR-197-3p	3.24E-03	0.4	479	73	189	13	551	480	405	198	196	174
942	hsa-miR-1260b_R-1	3.27E-03	0.5	212	28	105	9	237	218	182	115	97	103
564	hsa-miR-548av-3p_L+2	3.28E-03	0.2	43	3	7	2	44	39	46	6	5	8

517	hsa-miR-625-3p	3.42E-03	1.9	103	12	195	26	114	105	89	225	178	183
33	hsa-miR-3960_L-2R-2_1ss12AC	3.49E-03	7.7	158	53	1,213	534	185	193	97	1,823	979	836
474	hsa-miR-7706	3.63E-03	0.4	63	8	27	5	71	61	55	30	29	22
496	hsa-miR-671-3p	3.74E-03	0.3	184	29	54	12	216	178	158	60	61	39
592	hsa-miR-500a-3p_R+1	3.74E-03	0.3	405	34	139	26	411	435	367	114	167	136
473	hsa-miR-7974	3.85E-03	0.3	224	18	63	13	245	217	211	77	61	52
634	hsa-miR-4516_L-3R+1	3.89E-03	15.9	38	14	605	88	48	44	22	704	580	533
741	hsa-miR-331-5p_R-1	4.00E-03	0.8	330	15	263	12	336	341	313	277	260	253
586	hsa-miR-502-3p_R+2	4.07E-03	0.4	260	40	101	20	292	215	272	79	108	117
925	hsa-miR-128-1-5p	4.15E-03	0.4	56	13	21	4	71	48	49	20	25	18
669	hsa-miR-409-3p	4.22E-03	0.5	739	16	382	34	757	733	727	348	417	381
808	hsa-miR-23b-5p_L-1	4.47E-03	0.2	354	38	86	20	393	317	351	63	99	96
615	hsa-miR-4746-5p	4.61E-03	0.5	33	5	15	3	38	32	29	14	18	13
406	hsa-mir-3656-p3_1ss13AC	4.78E-03	6.5	13	5	86	16	17	14	8	103	82	71
635	hsa-miR-4508_L+2	4.86E-03	12.8	19	6	243	17	25	19	12	228	260	240
461	hsa-miR-9-3p	4.91E-03	0.4	34	5	14	3	29	39	33	11	13	17
950	hsa-miR-1249-3p	4.92E-03	0.4	73	15	26	6	88	72	59	30	29	20
730	hsa-miR-342-3p_R+1	5.08E-03	0.5	821	64	451	5	872	844	749	445	452	456
26	hsa-miR-450b-5p_R-1	5.11E-03	0.3	1,367	322	467	85	1,020	1,424	1,656	391	559	451
403	hsa-mir-3687-1-p5	5.65E-03	5.6	9	4	50	19	9	13	6	71	44	35
841	hsa-miR-195-5p_R+1	5.81E-03	2.3	21	2	48	9	22	19	22	43	43	58
358	hsa-mir-548i-2-p5_1ss8TA	5.85E-03	2.8	13	3	36	8	15	9	14	27	43	37
979	hsa-let-7a-3p_R+1	6.30E-03	0.5	456	83	208	26	363	481	523	179	217	228
534	hsa-miR-577_L+1	6.37E-03	0.4	71	4	25	5	75	69	70	21	25	30
445	hsa-mir-1248-p5_1ss14CA	6.72E-03	8.3	9	3	77	12	5	12	10	69	71	91
807	hsa-miR-24-1-5p_L+1	7.05E-03	0.4	113	22	49	7	121	130	88	57	43	47
582	hsa-miR-505-3p_L-1R+2	7.65E-03	0.5	275	9	132	18	283	277	265	153	123	120
756	hsa-miR-3196_R-3	7.81E-03	5.4	8	3	45	18	10	11	5	64	43	29
719	hsa-miR-361-5p	8.08E-03	0.5	788	139	363	30	794	924	645	376	328	384
888	hsa-miR-141-3p_R-1	8.20E-03	2.1	41	7	89	5	34	42	47	93	90	83
811	hsa-miR-2355-3p	8.24E-03	0.6	45	6	28	3	51	42	42	28	26	31

521	hsa-miR-615-3p_R-1	8.37E-03	0.2	93	12	17	7	105	82	91	12	25	14
777	hsa-miR-30e-3p	8.58E-03	0.6	870	21	479	51	870	891	849	510	506	420
785	hsa-miR-301a-5p	8.87E-03	0.4	74	7	29	6	79	66	77	22	31	34
776	hsa-miR-31-3p_R+1	8.95E-03	0.5	1,162	146	630	102	1,050	1,327	1,109	707	515	668
882	hsa-miR-147b_R-1	8.95E-03	4.8	187	14	900	279	186	202	174	1,214	681	805
627	hsa-miR-455-3p_R+1	9.01E-03	0.5	249	36	121	5	246	287	215	127	118	119
579	hsa-miR-532-3p	9.34E-03	0.6	34	3	19	3	37	32	33	20	22	17
409	hsa-mir-3648-2-p3	9.76E-03	1.8	48	8	88	13	49	56	40	103	81	79

Supplementary Table S3. Change in the numbers of reads of individual miR-34a isoforms in A549 cells after transfection with tRNA/mir-34a, as revealed by deep sequencing analysis. Cells treated with the same dose of tRNA/MSA were used as controls. There were triplicate treatments in each group that were sequenced separately.

cluster#=86 genomeSeqID=224589800 strand=- start=9211727 end=9211836 reads#=460284 mir#=16

genome ggccagctgtgagtgtttcttggcagtgtcttagctggttgttgtgagcaatagtaaggaagcaatcagcaagtatactgccctagaagtgctgcacgttgtggggccc

hsa-mir-34a ggccagctgtgagtgtttcttTGGCAGTGTCTTAGCTGGTTGTtgtgagcaatagtaaggaagCAATCAGCAAGTATACTGCCCTagaagtgctgcacgttgtggggccc

				Group 1								Group 2			
				MSA			tRNA/mir-34a			MSA		tRNA/mir-34a			
				#1	#2	#3	#1	#2	#3	Mean	SD	Mean	SD		
199_70386	TGGCAGTGTCTTAGCTGGTTGT		827,827,0,22,22,0,5	565	570	446	25,574	19,592	20,099	527	70	21,755	3,317		
209_65930	TGGCAGTGTCTTAGCTGGTTGTT		867,867,0,23,23,0,5	443	462	349	25,539	16,224	20,066	418	61	20,610	4,681		
219_63765		CACGTTGTGGGGCCC	550,550,0,15,15,0,3	34	38	21	1,616	2,065	2,182	31	9	1,954	299		
1858_6610	TGGCAGTGTCTTAGCTGGTTG		790,790,0,21,21,0,5	19	14	13	2,410	1,906	2,136	15	3	2,151	252		
2997_4110	TTTCTTTGGCAGTGTCTTAGC		789,789,0,21,21,0,5	23	20	14	966	1,407	1,541	19	5	1,305	301		
2253_5448	TGGCAGTGTCTTAGCTGGTT		749,749,0,20,20,0,5	3	1	5	3,345	979	1,093	3	2	1,806	1,334		
3141_3923		TGTTGTGAGCAATAGTAAGGAAGC	904,904,0,24,24,0,5	18	19	18	1,321	966	1,396	18	1	1,228	230		
3161_3894		AAGGAAGCAATCAGCAAGTATACT	908,908,0,24,24,0,3	1	0	1	1,312	957	1,616	1	1	1,295	330		
4125_2962	TTGGCAGTGTCTTAGCTGGTTGTT		907,907,0,24,24,0,5	3	4	2	1,053	802	1,072	3	1	976	151		
3539_3503		CAATCAGCAAGTATACTGCCCT	834,834,0,22,22,0,3	41	33	26	1,220	780	1,207	33	8	1,069	250		
5884_2064	CTGTGAGTGTTTCTTTGGCAGT		827,827,0,22,22,0,5	4	0	0	719	559	772	1	2	683	111		
6115_1971	GGCAGTGTCTTAGCTGGTTGTT		825,825,0,22,22,0,5	4	6	3	845	503	568	4	2	639	182		
8023_1485	TTGGCAGTGTCTTAGCTGGTTGT		867,867,0,23,23,0,5	4	3	2	499	429	526	3	1	485	50		
6513_1850		AGGAAGCAATCAGCAAGTATACT	868,868,0,23,23,0,3	0	0	0	767	406	676	0	0	616	188		
8071_1477		AGTAAGGAAGCAATCAGCAAGTATA	944,944,0,25,25,0,3	1	0	0	596	371	509	0	1	492	113		
8049_1480	TGGCAGTGTCTTAGCTGGTTGTTT		909,869,40,24,23,1,5	37	20	21	417	369	477	26	10	421	54		
12282_930	CCAGCTGTGAGTGTTTCTTTGGC		866,866,0,23,23,0,5	12	3	2	179	354	352	6	6	295	100		
6865_1752	TTGGCAGTGTCTTAGCTGGTT		790,790,0,21,21,0,5	2	1	0	965	348	427	1	1	580	336		
9120_1298	GCTGTGAGTGTTTCTTTGGCAGTG		901,901,0,24,24,0,5	0	0	2	588	325	383	1	1	432	138		
12156_940	TTGGCAGTGTCTTAGCTGGTTG		830,830,0,22,22,0,5	0	6	2	309	290	323	3	3	307	17		
15464_715	AGCTGTGAGTGTTTCTTTGGC		785,785,0,21,21,0,5	3	0	1	178	264	243	1	2	228	45		
9847_1195		GTAAGGAAGCAATCAGCAAGTATACT	983,983,0,26,26,0,3	0	0	1	478	258	457	0	1	398	121		

9558_1233	AGGAAGCAATCAGCAAGTATACTG	911,911,0,24,24,0,3	0	1	1	598	252	381	1	1	410	175
12787_889	TTTCTTTGGCAGTGTCTTAGCT	830,830,0,22,22,0,5	6	2	7	317	226	301	5	3	281	49
15808_697	CCAGCTGTGAGTGTTTCTTTGGCAGTGTCT	1141,1141,0,30,30,0,5	0	6	1	208	222	240	2	3	223	16
16195_678	GTTTCTTTGGCAGTGTCTTAGC	817,817,0,22,22,0,5	1	4	1	196	216	252	2	2	221	28
14992_740	AGTGTTTCTTTGGCAGTG	661,661,0,18,18,0,5	1	0	1	282	213	242	1	1	246	35
11462_1006	CAATCAGCAAGTATACTGCCCTT	874,834,40,23,22,1,3	2	5	1	413	212	343	3	2	323	102
15061_737	CTGGTTGTTGTGAGCAATA	710,710,0,19,19,0,5	9	7	14	218	211	208	10	4	212	5
10575_1103	TGGCAGTGTCTTAGCTGGTTGTA	866,827,39,23,22,1,5	7	12	5	512	208	321	8	4	347	154
11686_983	TTTGGCAGTGTCTTAGCTGGTT	828,828,0,22,22,0,5	0	0	0	494	202	285	0	0	327	150
12446_918	AGCTGTGAGTGTTTCTTTGGCAGTG	940,940,0,25,25,0,5	1	0	0	418	201	298	0	1	306	109
19828_541	CAAGTATACTGCCCT	550,550,0,15,15,0,3	1	3	1	92	197	222	2	1	170	69
18517_585	CCCTAGAAGTGCTGC	549,549,0,15,15,0,3	0	2	1	142	197	227	1	1	189	43
16185_679	CCAGCTGTGAGTGTTTCTTTGGCAGT	987,987,0,26,26,0,5	1	1	0	154	197	308	1	1	220	79
20466_522	GTGAGTGTTTCTTTGGCAGT	740,740,0,20,20,0,5	0	1	0	132	196	186	0	1	171	34
14767_753	AAGGAAGCAATCAGCAAGTATACTG	951,951,0,25,25,0,3	0	0	0	308	193	251	0	0	251	58
15609_707	CTGTGAGTGTTTCTTTGGCAGTG	864,864,0,23,23,0,5	1	0	0	209	191	304	0	1	235	61
16465_665	GGGCAGTGTCTTAGCTGGTTGT	771,748,23,22,21,1,5	4	3	7	256	190	190	5	2	212	38
17279_632	CAGCTGTGAGTGTTTCTTTGGCAGTGTCT	1100,1100,0,29,29,0,5	3	0	0	177	189	250	1	2	205	39
19544_550	CCCTAGAAGTGCTGCAC	629,629,0,17,17,0,3	1	0	3	143	187	210	1	2	180	34
2243_5472	CTGCACGTTGTGGGGCC	627,627,0,17,17,0,3	13	18	17	161	180	221	16	3	187	31
18258_594	CCCTAGAAGTGCTGCACG	669,669,0,18,18,0,3	1	3	1	166	179	238	2	1	194	38
16340_671	TTTGGCAGTGTCTTAGCTGGTTGTT	947,947,0,25,25,0,5	1	0	1	248	174	244	1	1	222	42
19816_542	CTGTGAGTGTTTCTTTGGCAGTGTCT	980,980,0,26,26,0,5	8	3	5	143	172	180	5	3	165	19
20352_525	CAGCTGTGAGTGTTTCTTTGGC	830,830,0,22,22,0,5	9	3	3	130	168	188	5	3	162	29
20551_520	TTTGGCAGTGTCTTAGCTGGTTGT	909,909,0,24,24,0,5	1	1	0	190	168	157	1	1	172	17
17308_631	GGGCAGTGTCTTAGCTGGTTGTT	805,783,22,23,22,1,5	7	0	1	259	166	179	3	4	201	50
17877_608	CTGTGAGTGTTTCTTTGGCA	748,748,0,20,20,0,5	0	0	0	159	166	275	0	0	200	65
20117_533	ACTGCCCTAGAAGTGCTGCACGTT	905,905,0,24,24,0,3	0	0	0	165	158	209	0	0	177	28
16429_667	AATCAGCAAGTATACTGCCCT	793,793,0,21,21,0,3	4	7	6	217	157	232	6	2	202	40
23990_438	CTGTGAGTGTTTCTTTGGCAGTGT	902,902,0,24,24,0,5	0	0	0	139	156	138	0	0	144	10
2551_4833	CTGCACGTTGTGGGGCCC	667,667,0,18,18,0,3	27	19	17	170	154	188	21	5	171	17
21579_493	TGAGTGTTTCTTTGGCAGT	708,708,0,19,19,0,5	1	0	1	121	153	213	1	1	162	47

21970_483	TGTTTCTTTGGCAGTGTCTTAGC	866,866,0,23,23,0,5	7	4	6	135	152	165	6	2	151	15
27603_374	AGTGTTTCTTTGGCA	548,548,0,15,15,0,5	0	0	0	61	150	152	0	0	121	52
18312_592	TGGTTGTTGTGAGCAATA	666,666,0,18,18,0,5	0	1	1	239	144	195	1	1	193	48
24308_432	CTGTGAGTGTTTCTTTGGCAGTGTCTTAGCTGGTT	1340,1340,0,35,35,0,5	0	0	0	137	142	150	0	0	143	7
25501_409	CTGTGAGTGTTTCTTTGGCAGTGTCTT	1014,1014,0,27,27,0,5	6	0	1	117	141	132	2	3	130	12
23474_449	TGAGTGTTTCTTTGGC	588,588,0,16,16,0,5	1	5	1	109	140	166	2	2	138	29
17369_629	GCAAGTATACTGCCCTAGAAGTGCTG	981,981,0,26,26,0,3	0	0	0	242	140	246	0	0	209	60
24726_424	CCCTAGAAGTGCTGCA	588,588,0,16,16,0,3	0	2	1	107	138	166	1	1	137	30
23722_443	AGTGTTTCTTTGGCAGT	624,624,0,17,17,0,5	2	1	0	100	137	194	1	1	144	47
14227_786	CCAGCTGTGAGTGTTTCTTTGGCAGTG	1024,1024,0,27,27,0,5	0	0	0	390	137	256	0	0	261	127
21657_491	ATACTGCCCTAGAAGTGCTGCACGTT	987,987,0,26,26,0,3	1	0	2	175	137	175	1	1	162	22
22677_467	CTGTGAGTGTTTCTTTGGC	706,706,0,19,19,0,5	4	1	1	131	136	186	2	2	151	30
25657_407	TTTCTTTGGCAGTGTCT	625,625,0,17,17,0,5	2	7	3	80	133	148	4	3	120	36
29846_342	TTTCTTTGGCAGTGTCTTAGCTGGTTGTTGT	1181,1181,0,31,31,0,5	1	3	1	91	127	101	2	1	106	19
28036_367	TCTTAGCTGGTTGTTG	588,588,0,16,16,0,5	1	0	0	97	127	140	0	1	121	22
24285_432	GCTGTGAGTGTTTCTTTGGC	746,746,0,20,20,0,5	2	1	2	181	126	113	2	1	140	36
27340_378	CCAGCTGTGAGTGTTTCTTTG	792,792,0,21,21,0,5	0	1	0	94	124	156	0	1	125	31
22074_481	TTTCTTTGGCAGTGTCTTAGCTGGTTGTT	1108,1108,0,29,29,0,5	1	3	0	165	123	170	1	2	153	26
14734_755	AGTAAGGAAGCAATCAGCAAGTATACT	1021,1021,0,27,27,0,3	0	0	0	355	123	276	0	0	251	118
28049_367	TGAGTGTTTCTTTGGCAGTGT	785,785,0,21,21,0,5	0	1	0	107	122	133	0	1	121	13
17417_627	TGGCAGTGTCTTAGCTGGT	708,708,0,19,19,0,5	5	3	2	314	121	159	3	2	198	102
25729_405	AGTGTTTCTTTGGCAGTGTCTTAGCTGGTT	1137,1137,0,30,30,0,5	1	0	1	167	120	112	1	1	133	30
20578_519	AAGGAAGCAATCAGCAAGTATACTGCCCT	1114,1114,0,29,29,0,3	0	1	0	224	118	174	0	1	172	53
21535_494	GAAGCAATCAGCAAGTATACTGCCCT	994,994,0,26,26,0,3	1	0	0	173	117	202	0	1	164	43
26475_392	TGCCCTAGAAGTGCTGCACGTT	828,828,0,22,22,0,3	1	0	0	97	117	174	0	1	129	40
26045_400	AGTGTTTCTTTGGCAGTGTCT	782,782,0,21,21,0,5	7	7	5	98	116	128	6	1	114	15
32465_309	TGAGTGTTTCTTTGGCA	632,632,0,17,17,0,5	1	1	3	53	112	134	2	1	100	42
23084_457	CAAGTATACTGCCCTAGAAGTGCTG	952,952,0,25,25,0,3	1	0	0	167	112	176	0	1	152	35
31169_325	CCCTAGAAGTGCTGCACGTTG	792,792,0,21,21,0,3	1	0	0	90	111	120	0	1	107	15
29299_349	TGAGTGTTTCTTTGGCAGTGTCT	865,865,0,23,23,0,5	4	2	2	97	110	126	3	1	111	15
11822_969	AGAAGTGCTGCACGTTGTGGGGC	871,871,0,23,23,0,3	1	2	0	218	110	159	1	1	162	54
25961_402	TGAGTGTTTCTTTGGCAGTG	744,744,0,20,20,0,5	0	0	0	145	109	144	0	0	133	21

29343_349	TTTGGCAGTGTCTTAGCTGGTTG	870,870,0,23,23,0,5	0	0	1	105	108	133	0	1	115	15
21296_500	CAATCAGCAAGTATACTGCC	752,752,0,20,20,0,3	0	1	0	217	107	175	0	1	166	56
24756_423	AGTGTTTCTTTGGCAGTGTCTT	821,821,0,22,22,0,5	7	3	4	126	105	152	5	2	128	24
29488_347	TTGGCAGTGTCTTAGC	593,593,0,16,16,0,5	5	3	1	82	105	117	3	2	101	18
32540_309	CCCTAGAAGTGCTGCACGTT	749,749,0,20,20,0,3	1	2	2	74	105	113	2	1	97	21
33009_304	TTCTTTGGCAGTGTCTTAGC	747,747,0,20,20,0,5	3	1	1	61	105	110	2	1	92	27
30145_338	TTTCTTTGGCAGTGTCTTAGCTGGTTGTTGTG	1221,1221,0,32,32,0,5	2	2	1	84	104	130	2	1	106	23
29941_341	CAAGTATACTGCCCTAGAAGTGCT	906,906,0,24,24,0,3	0	1	1	91	104	128	1	1	108	19
27312_379	AAGCAATCAGCAAGTATACTGCCCT	946,946,0,25,25,0,3	0	0	0	128	104	143	0	0	125	20
29551_346	AGTATACTGCCCTAGAAGTGCTG	869,869,0,23,23,0,3	0	0	0	110	104	130	0	0	115	14
23030_458	GTAAGGAAGCAATCAGCAAGTATA	903,903,0,24,24,0,3	1	0	0	171	103	180	0	1	151	42
32885_305	TGAGTGTTTCTTTGGCAGTGTCTTAGCTGGTT	1223,1223,0,32,32,0,5	0	1	1	102	101	99	1	1	101	2

Supplementary Table S4. Comparison of the tRFs derived from tRNA/MSA and tRNA/mir-34a in A549 cells. The numbers of reads were determined by deep sequencing analysis of small RNAs isolated from A549 cells at 48 h post-transfection. There were triplicate treatments in each group that were sequenced separately.

			tRNA/MSA					tRNA/mir-34a				
readID	sequence	length	MSA-1	MSA-2	MSA-3	Mean_MSA	SD_MSA	34a-1	34a-2	34a-3	Mean_34a	SD_34a
97_175156	AATCCCGTCGTAGCCACCA	19	18,509	16,811	14,031	16,450	2,261	14,164	11,412	15,511	13,696	2,089
100_165108	AGTTGGTTAGAGCAGCGGCC	20	11,212	14,145	23,263	16,207	6,284	11,875	9,187	10,969	10,677	1,368
132_110254	GTTCGAATCCCGTCGTAGCC	20	10,070	12,781	21,280	14,710	5,849	11,053	6,396	6,742	8,064	2,595
172_80912	CCACAGGTTCGAATCCCGTCGTAGCCACCA	30	11,033	15,934	11,708	12,892	2,656	2,949	1,439	3,712	2,700	1,157
121_121817	AATCCCGTCGTAGCC	15	8,942	11,485	18,120	12,849	4,739	11,406	13,026	11,075	11,836	1,044
309_44558	TTCGAATCCCGTCGTAGCCACC	22	12,394	10,237	8,148	10,260	2,123	2,228	1,340	1,675	1,748	448
156_90312	AGTTGGTTAGAGCAGCGGCCG	21	8,664	7,962	10,457	9,028	1,287	6,978	4,367	5,385	5,577	1,316
127_115481	AGTTGGTTAGAGCAGCGGC	19	5,344	7,713	13,769	8,942	4,345	3,046	3,137	3,869	3,351	451
186_76451	ATCCCGTCGTAGCCACCA	18	7,780	7,081	5,957	6,939	920	6,726	5,876	7,408	6,670	768
330_42074	ACAGGTTCGAATCCCGTCGTAGCCACCA	28	5,602	7,549	5,676	6,276	1,103	2,246	997	2,698	1,980	881
434_29086	TCGATGGTTGCGGCC	15	1,167	3,821	12,959	5,982	6,186	639	599	584	607	28
344_40554	CACAGGTTCGAATCCCGTCGTAGCCACCA	29	4,966	7,162	5,293	5,807	1,185	1,906	1,037	2,326	1,756	657
192_74219	AGTTGGTTAGAGCAGCGGCCGAG	23	6,141	5,273	4,595	5,336	775	4,093	3,193	4,889	4,058	849
674_18378	CGATGGTTGCGGCCG	15	577	4,793	10,374	5,248	4,914	47	43	43	44	2
322_43379	AGTTGGTTAGAGCAGCG	17	1,703	3,651	10,162	5,172	4,430	531	628	805	655	139
853_14431	ACGGTGACGTCGATG	15	824	4,569	9,018	4,804	4,102	2	1	2	2	1
256_55421	GAATCCCGTCGTAGCCACCA	20	5,428	4,662	3,990	4,693	720	4,630	3,254	4,460	4,115	750
362_38640	AGTTGGTTAGAGCAGCGG	18	2,049	4,041	7,416	4,502	2,713	615	573	842	677	145
372_36052	TTCGAATCCCGTCGTAGCCACCA	23	5,149	4,048	3,321	4,173	920	4,348	1,908	3,060	3,105	1,221
988_12449	ACGGTGACGTCGATGGTTGCGGCC	24	3,413	4,184	4,831	4,143	710	3	1	4	3	2
232_61240	CCCGTCGTAGCCACCA	16	4,240	4,075	3,566	3,960	351	4,565	4,200	5,281	4,682	550
284_49613	CGAATCCCGTCGTAGCCACCA	21	3,765	4,209	3,300	3,758	455	4,359	2,956	4,000	3,772	729
304_44885	TCCCGTCGTAGCCACCA	17	4,027	3,718	3,304	3,683	363	4,198	3,444	4,710	4,117	637
491_25688	TCGAATCCCGTCGTAGCC	18	1,887	2,918	5,590	3,465	1,911	3,077	2,032	2,068	2,392	593
485_25857	AGTTGGTTAGAGCAGCGGCCGAGT	24	3,926	3,562	2,669	3,386	647	839	939	1,230	1,003	203
404_32520	GTTCGAATCCCGTCGTAGCCACCA	24	3,970	3,495	2,628	3,364	680	3,259	1,679	2,759	2,566	808
189_75563	GGCTACGTAGCTCAGTTGGTTAGAGCAGCGGC	32	2,904	3,775	3,290	3,323	436	13,278	3,407	3,721	6,802	5,611
592_21322	TCACAGGTTCGAATCCCGTCGTAGCCACCA	30	2,882	3,974	3,063	3,306	585	835	362	1,100	766	374
707_17387	GTTCGAATCCCGTCGTAGCCACC	23	4,076	3,102	2,268	3,149	905	845	614	743	734	116
454_27689	TCGAATCCCGTCGTAGCCACCA	22	3,710	3,321	2,391	3,141	678	2,512	1,237	1,911	1,887	638
498_25322	AATCCCGTCGTAGCCACC	18	3,097	2,748	2,107	2,651	502	2,209	1,724	1,972	1,968	243
1020_12068	GTTCGAATCCCGTCGTAG	18	676	2,005	4,778	2,486	2,093	321	264	398	328	67
943_12979	TCGAATCCCGTCGTAGCCACC	21	2,806	2,259	1,665	2,243	571	1,250	770	796	939	270
1967_6275	ACGGTGACGTCGATGG	16	381	1,889	4,002	2,091	1,819	0	0	0	0	0

408_31904	GGCTACGTAGCTCAGTTGGTTAGAGCAGCG	30	1,944	2,105	1,913	1,987	103	1,728	1,384	1,989	1,700	303
1068_11548	ACAGGTTCGAATCCCGTCGTAGCCACC	27	1,959	2,060	1,540	1,853	276	495	340	598	478	130
1504_8185	AGGTTCGAATCCCGTCGTAGCCACC	25	1,906	2,122	1,442	1,823	347	548	312	465	442	120
815_15076	CCACAGGTTCGAATCCCGTCGTAGCCACC	29	1,769	1,967	1,474	1,737	248	495	272	598	455	167
1678_7393	TCGATGGTTGCGGCCG	16	221	1,394	3,534	1,716	1,680	98	53	80	77	23
1217_10133	CACAGGTTCGAATCCCGTCGTAGCCACC	28	1,719	1,887	1,386	1,664	255	336	235	467	346	116
1485_8270	TTCGAATCCCGTCGTAGCCACT	22	1,926	1,530	1,310	1,589	312	763	529	616	636	118
2136_5768	TTCGAATCCCGTCGTAGCCACCT	23	1,939	1,608	1,062	1,536	443	53	52	61	55	5
2676_4580	ACGGTGACGTCGATGGTT	18	1,320	1,732	1,523	1,525	206	1	1	1	1	0
1078_11483	CCCGTCGTAGCCACC	15	1,656	1,499	1,417	1,524	121	758	660	784	734	65
701_17510	GAATCCCGTCGTAGCC	16	1,200	1,444	1,877	1,507	343	2,137	2,077	1,750	1,988	208
976_12522	ATCCCGTCGTAGCCACC	17	1,712	1,532	1,245	1,496	236	909	858	939	902	41
2741_4474	ACGGTGACGTCGATGGTTGCGGC	23	902	1,423	2,135	1,487	619	1	0	2	1	1
840_14648	CGAATCCCGTCGTAGCCACC	20	1,740	1,483	1,209	1,477	266	2,067	1,507	1,798	1,791	280
1982_6212	GTTCGAATCCCGTCGTA	17	215	1,160	2,917	1,431	1,371	323	119	137	193	113
996_12353	CAGTTGGTTAGAGCAGCGGCC	21	1,018	1,209	1,697	1,308	350	758	549	696	668	107
543_23228	CCGTCGTAGCCACCA	15	1,196	1,508	1,193	1,299	181	2,020	1,881	2,553	2,151	355
1407_8727	GTTCGAATCCCGTCGTAGC	19	373	1,281	2,150	1,268	889	763	458	399	540	195
1070_11517	CAGTTGGTTAGAGCAGCGGC	20	680	1,009	1,594	1,094	463	282	274	328	295	29
1178_10503	AATCCCGTCGTAGCCA	16	779	944	1,320	1,014	277	751	669	872	764	102
769_16123	GGCTACGCAGCTCAGTTGGTTAGAGCAGCGGC	32	944	761	810	838	95	3,594	852	759	1,735	1,611
636_19945	GTTGTGGGGCCCAAGA	16	941	927	619	829	182	1,029	3,112	3,376	2,506	1,286
761_16355	AGTTGGTTAGAGCAGCGGCCGAGTA	25	849	894	662	802	123	821	1,177	1,459	1,152	320
824_14994	CAGGTTCGAATCCCGTCGTAGCCACCA	27	631	860	592	694	145	1,182	779	1,222	1,061	245
1830_6759	TTGGTTAGAGCAGCGGCCGAGTA	23	299	268	229	265	35	969	947	1,334	1,083	217
1588_7759	GGTTAGAGCAGCGGCCGAGTA	21	191	202	222	205	16	1,286	1,247	1,818	1,450	319
2671_4597	CTCAGTTGGTTAGAGCAGCGGCCGAGTA	28	151	156	123	143	18	1,072	1,016	1,454	1,181	238
2445_5084	GTCTTAGCTGGTTGTT	16	83	93	95	90	6	1,526	1,053	1,512	1,364	269
3295_3739	TAGCTCAGTTGGTTAGAGCAGCGGCCGAGTA	31	35	37	51	41	9	761	988	1,383	1,044	315
1700_7279	ACGTGGACCGGCCAGCT	17	23	14	16	18	5	2,095	2,461	2,502	2,353	224
1763_7005	CCGAGTAATTTACGTCGACGTGGA	24	18	20	8	15	6	1,517	2,659	2,620	2,265	648
2853_4299	CCGAGTAATTTACGTCGACGTGGAC	25	15	16	13	15	2	1,366	1,428	1,378	1,391	33
2590_4742	ACGTGGACCGGCCAGC	16	10	16	13	13	3	1,279	1,570	1,713	1,521	221
2460_5055	CGACGTGGACCGGCCAGCT	19	14	1	11	9	7	1,655	1,627	1,675	1,652	24
3625_3427	CGACGTGGACCGGCCAGC	18	6	7	10	8	2	1,016	1,117	1,213	1,115	99
3715_3330	CGACGTGGACCGGCCAGCTGTGAGT	25	8	2	3	4	3	934	1,194	1,152	1,093	140
1769_6962	TGGACCGGCCAGCTGTGAGTGTTTCTTTGGCAGTG	35	0	0	1	0	1	1,670	2,569	2,693	2,311	558